**Table 4.1:** Data of Three-area Loop Interconnected Power System (Area Capacity Ratio 5:10:2)

System Parameters	Area 1	Area 2	Area 3
Inertia Constant (MW.s Hz)	$M_1 = 0.2$	$M_2 = 0.0167$	$M_3 = 0.15$
Damping Coefficient (MW/Hz)	$D_1 = 0.006$	$D_2 = 0.00833$	$D_3 = 0.005$
Turbine Time Constant (s)	$T_{i1} = 0.25$	$T_{i2} = 0.3$	$T_{r_3} = 0.25$
Governor Time Constant (s)	$T_{g1}=0.1$	$T_{g2} = 0.08$	$T_{g3} = 0.1$
Regulation Ratio (Hz/MW)	$R_1 = 2.4$	$R_2 = 2.4$	$R_{3}=2.4$
Bias Coefficient (MW/Hz)	$B_1 = 0.5$	$\overline{B_2} = 0.5$	$B_{1} = 0.5$
Integral Controller  Gain (1/s)	$K_{ii} = 0.5$	K <sub>12</sub> = 0.5	$K_{i3}=0.\overline{5}$
Synchronizing Power Coefficient (MW/rad)	$T_{12} = 0.159$ , $T_{23} = 0.064$ , $T_{31} = 0.079$		
Area Capacity Ratio	$a_{12} = 2.0$ , $a_{23} = 0.2$ , $a_{31} = 2.5$		

To exhibit the results of system reduction by overlapping decompositions, Table 4.2 shows eigenvalues of the original systems (4.1) in comparison to design subsystems (4.11) and (4.12). The damping ratio and oscillation frequency of the corresponding oscillation mode in the design subsystems are nearly equal to those of the original system. This reveals that the design subsystems (4.11) and (4.12) retain the physical characteristic of the original system (4.1).

Table 4.2: Eigenvalues of Original System and Design Subsystems Before and After the Overlapping Decompositons

Original System (4.1)	Subsystem (4.11)	Subsystem (4.12)
$\lambda_1 = -0.0415$	-	-
$\lambda_{2,i} = -0.0173 \pm j4.365$	$\lambda_{2,1} = -0.015 \pm j3.53$	-
$(\zeta = 0.0035, f = 0.695 Hz)$	$(\zeta = 0.0043, f = 0.562 Hz)$	
$\lambda_{4.5} = -0.0185 \pm j3.291$	-	$\lambda_{4,5} = -0.0167 \pm j3.31$
$(\zeta = 0.0056, f = 0.524 Hz)$		$(\zeta = 0.005, f = 0.527 Hz)$

As experimental results, the optimally tuned parameters of designed frequency stabilizers in (4.11) and (4.12) are obtained as given in Table 4.3. Note that the optimized frequency stabilizer based on (4.18) is referred to as "Robust frequency stabilizer".

Table 4.3: Parameters of Robust Frequency Stabilizers

Designed Robust					
Frequency Stabilizer	K	$T_{i}$	<i>T</i> <sub>2</sub>	<i>T</i> ,	<i>T</i> <sub>4</sub>
SSSC12	0.2188	0.2587	0.0158	0.0575	0.2316
SSSC23	0.2378	1.5025	0.5386	1.6268	0.5075

For comparison purposes, the second-order lead/lag frequency stabilizer in (4.11) and (4.12) are also designed with the same design specification, which requires the same damping ratio  $\zeta_{destred} = 0.25$ . The control parameters  $K, T_1, T_2, T_3$ , and  $T_4$  are searched by TS via the optimization problem (4.20). Note that the robust stability index term  $(\gamma)$  is excluded.

Minimize 
$$F(K,T_i) = \alpha$$
  
Subject to  $K_{\min} \le K \le K_{\max}$  (4.20)  
 $T_{i,\min} \le T_i \le T_{i,\max}$ ,  $i = 1,...,4$ 

Here, the optimized frequency stabilizer based on (4.20) is referred to as "Non-robust frequency stabilizer". Table 4.4 shows the control parameters of the non-robust frequency stabilizer.

Table 4.4: Parameters of Non-Robust Frequency Stabilizers

Designed Non-robust					
Frequency Stabilizer	K	$T_{i}$	<i>T</i> <sub>2</sub>	$T_3$	<i>T</i> <sub>4</sub>
SSSC12	4.2863	0.1344	1.0011	1.0978	1.3807
SSSC23	4.3683	0.1344	0.9933	1.3467	1.3802

Table 4.5 shows eigenvalues of subsystems (4.11) and (4.12) in case of SSSCs with robust frequency stabilizers installed in comparison with a case of SSSCs with no frequency stabilizer and a case of SSSCs with non-robust frequency stabilizers installed. The results describe that the damping ratios of the eigenvalues corresponding to the desired inter-area modes are improved to 0.25, as design specification.

Table 4.5: Comparison of Eigenvalues of Design Subsystems

			SSSC With Robust
Design Subsystem	SSSC with No	SSSC With Non-	Frequency
	Frequency Stabilizer	Robust Frequency	Stabilizer
		Stabilizer	
G <sub>s1</sub>	$-0.015 \pm j3.53$	$-1.8369 \pm j7.1143$	$-0.6093 \pm j2.3595$
	$\zeta = 0.0043$	$\zeta = 0.25$	ζ = 0.25
G,2	$-0.0167 \pm j3.31$	-1.667 ± j6.4559	-0.3534 ± j1.3685
	ζ = 0.005	ζ = 0.25	<i>ζ</i> = 0.25

Next, the MSM is used to evaluate the robust stability margin of system (4.11) and (4.12) included with each frequency stabilizer. As shown in Table 4.6, the value of MSM in case of the system with robust frequency stabilizer is greater than that in case of the system with non-robust stabilizer. This clearly signifies that the better robust stability margin of the power system incorporated with robust frequency stabilizer can be achieved by the optimization problem (4.18).

Table 4.6: Comparison of MSM

System	With Non-Robust Frequency Stabilizer	With Robust Frequency Stabilizer
$G_{s_1}$	0.5151	0.71430
$G_{s_2}$	0.5332	0.61240

Table 4.7 shows the eigenvalues of the original system (4.1) before and after control. After each frequency stabilizer is included in the system, the damping ratios of the corresponding inter-area modes are enhanced as expected. This confirms the merit of overlapping decompositions that if the subsystems are stabilized by their own control inputs, the stability of the original system can be guaranteed.

Table 4.7: Comparison of Eigenvalues of Original System

Inter-Area Oscillation Mode	No Frequency Stabilizer	With Non-Robust Frequency Stabilizer	With Robust Frequency Stabilizer
Between Areas	$-0.0173 \pm j4.365$ $\zeta = 0.0035$	$-1.7631 \pm j7.6011$ $\zeta = 0.226$	$-0.6619 \pm j2.898$ $\zeta = 0.223$
Between Areas 2 and 3	$-0.0185 \pm j3.291$ $\zeta = 0.0056$	$-1.6716 \pm j6.4702$ $\zeta = 0.25$	$-0.3596 \pm j1.376$ $\zeta = 0.253$

Here, the performance and robustness of the designed frequency stabilizers are evaluated in a linearized model of the three-area interconnected system. Here, changing load disturbances which are simultaneously applied to areas 1 and 3, are composed of three different components in the frequency domain, one of which (underlined component) has a frequency corresponding to the inter-area mode of interest (see Table 4.6), as follows.

Area 1 : 
$$\Delta P_{t1} = 0.003\sin(4.36t) + 0.005\sin(5.3t) - 0.007\sin(6t)$$
 (4.21)

Area 3: 
$$\Delta P_{L3} = 0.003\sin(3.29t) + 0.007\sin(4t) - 0.005\sin(4.5t)$$
 (4.22)

Note that the dynamic of governor as illustrated in Fig. 4.9, is also included into each area in this simulation study. Table 4.8 shows operating conditions and applied disturbances.

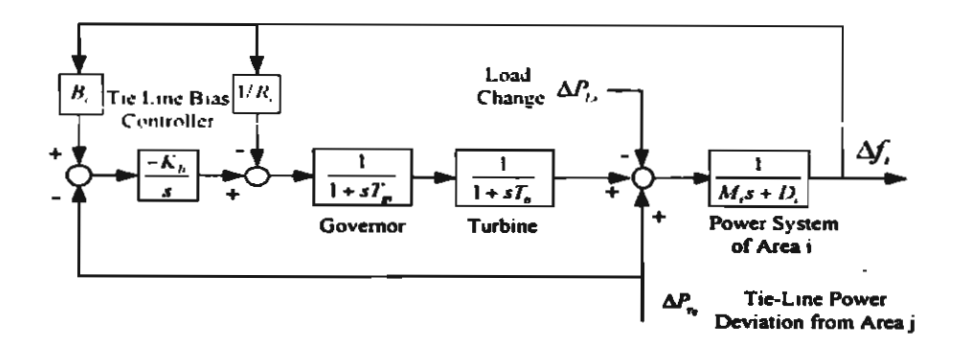


Figure 4.9: Linearized system model of area i including governor

Table 4.8: System Conditions and Applied Disturbances

Case	Disturbances	
1	At normal (design) condition, $\Delta P_{L1}$ is applied to area 1 and $\Delta P_{L3}$ is	
	applied to area 3. (No parameter variations)	
2	At unstable condition, $\Delta P_{L1}$ is applied to area 1 and $\Delta P_{L3}$ is applied at area 3 while damping coefficients $D_1$ and $D_3$ are set -0.45.	

For case 1, the damping effect of each designed stabilizer is investigated. As demonstrated in Figs. 4.10 – 4.12, both robust and non-robust frequency stabilizers are able to damp the frequency oscillation in each area, effectively. In addition, Figs. 4.13 – 4.14 depict that both tie-lines 1-2 and 2-3 power oscillations are also stabilized by both frequency stabilizers. Nevertheless, the damping effect of the robust frequency stabilizer is better than that of the non-robust case. As declared in Figs. 4.15 and 4.16, the power output deviation of the robust frequency stabilizer for each SSSC is less or equal to that of non-robust frequency stabilizer.

In case 2, not only damping effect but also robust stability of the system incorporated with each frequency stabilizer are evaluated. It is assumed that both power systems 1 and 3 are in unstable conditions, so that  $D_1$  and  $D_3$  are set to -0.45 (MW/Hz). As the load disturbances applied to both areas, frequency deviations of areas 1, 2 and 3 in case of the nonrobust frequency stabilizer severely fluctuate and finally diverge as depicted in Figs. 4.17 – 4.19. Note that frequency deviation of each area in case of SSSCs without frequency

stabilizers (not shown here) also heavily oscillates and finally diverges. On the other hand, frequency oscillations in all areas are completely stabilized by the robust frequency stabilizer. The interconnected power system can maintain the system stability. Figures 20 and 21 also exhibit the significant damping effects of robust frequency stabilizers on the tie-lines 1-2 and 2-3 power oscillations. The power output deviations of robust frequency stabilizers are illustrated in Figs. 4.22 and 4.23. These simulation results confirm that under severe load disturbances and negative damping, the robustness of robust frequency stabilizer against such system uncertainties is considerably superior to that of non-robust frequency stabilizer.

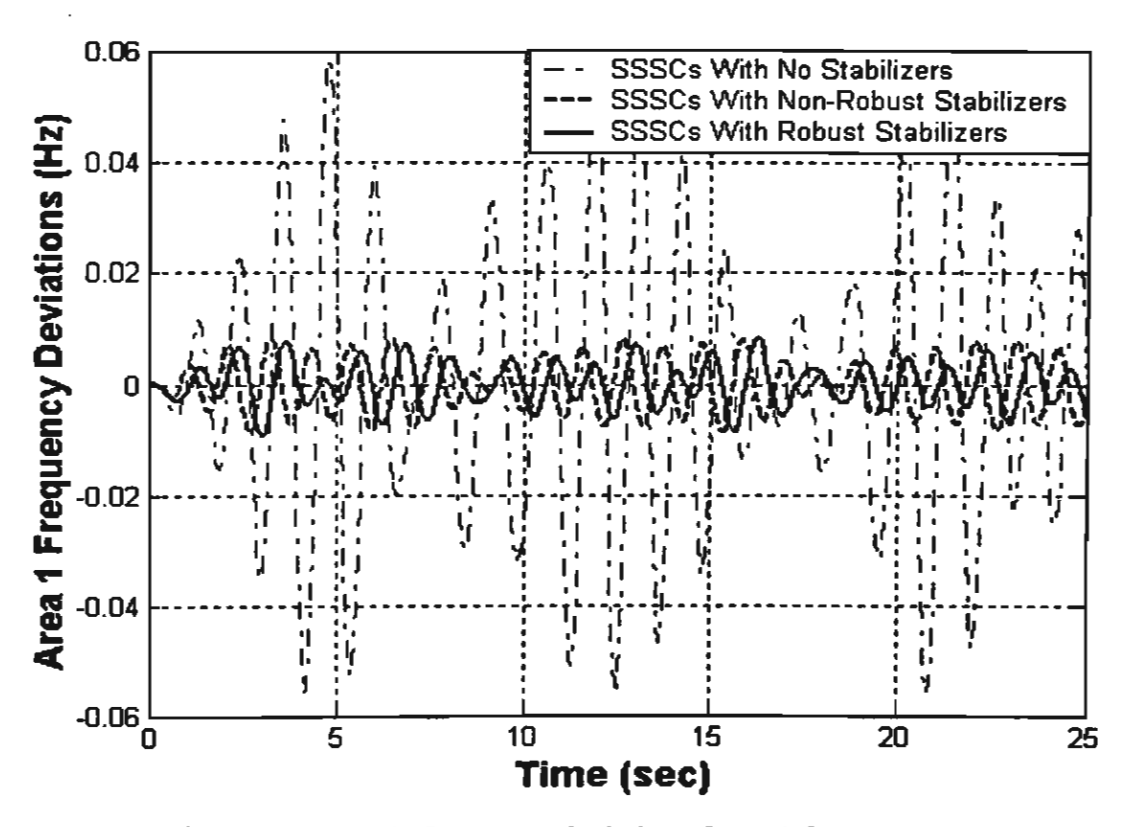


Figure 4.10: Frequency deviation of area 1 for case 1

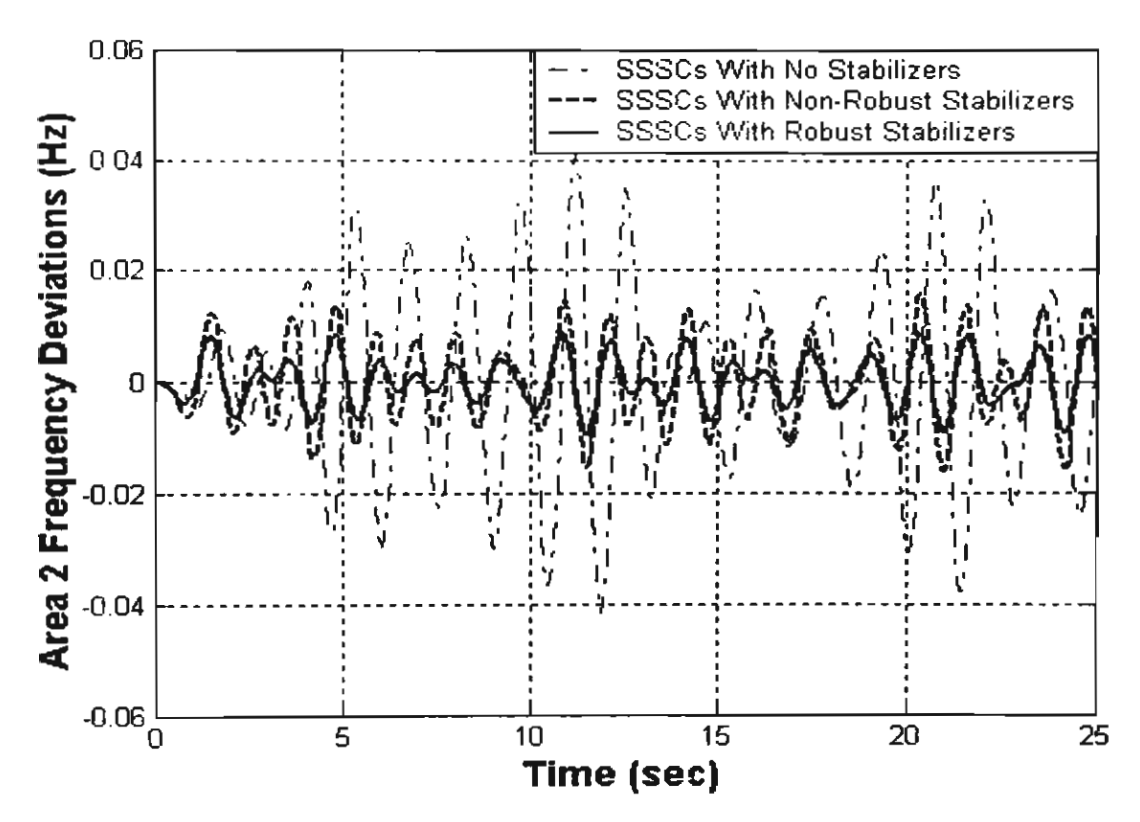


Figure 4.11: Frequency deviation of area 2 for case 1

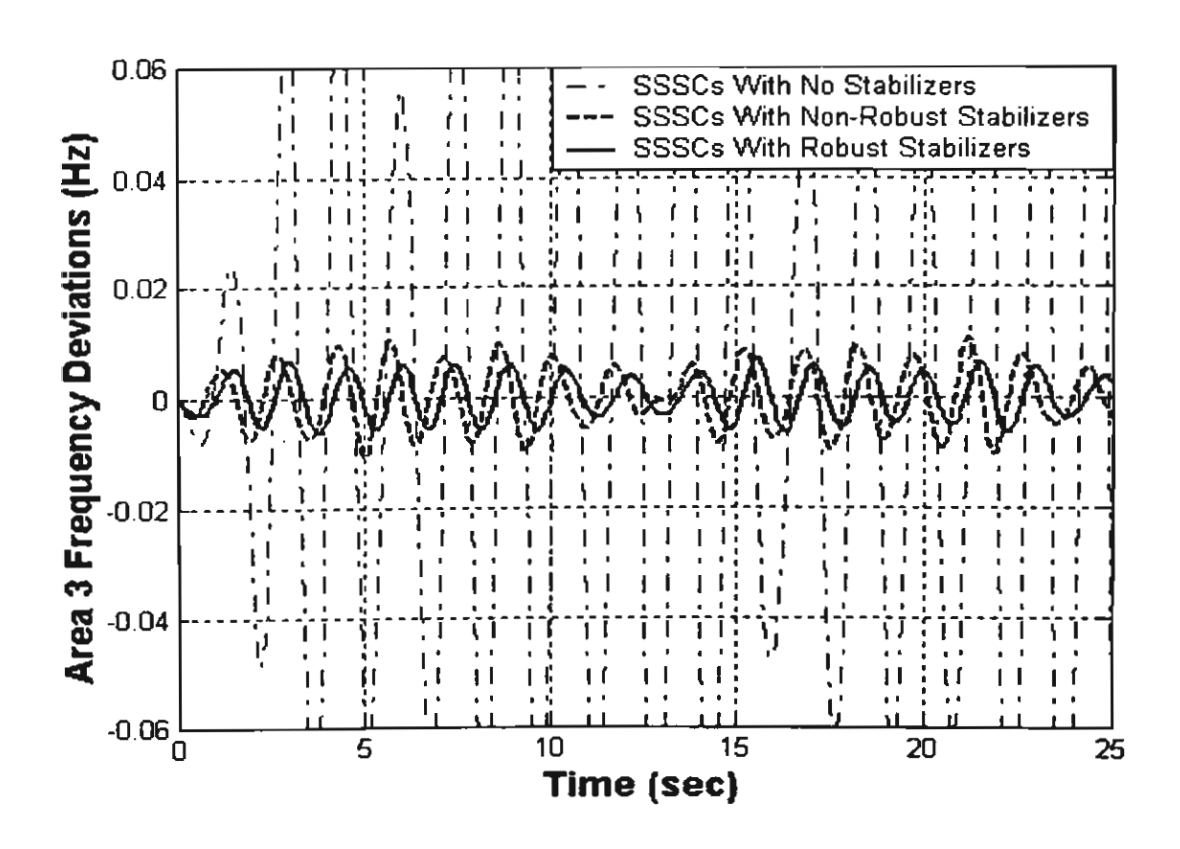


Figure 4.12: Frequency deviation of area 3 for case 1

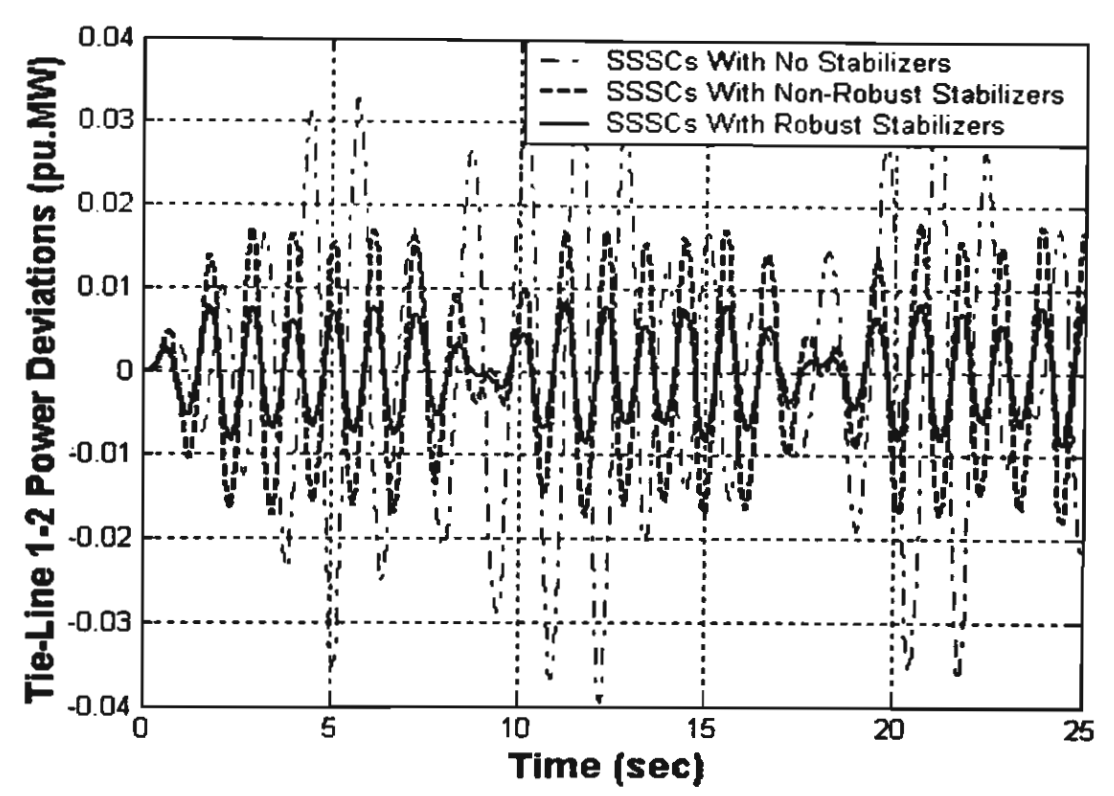


Figure 4.13: Tie-line power deviation between areas 1 and 2 for case 1

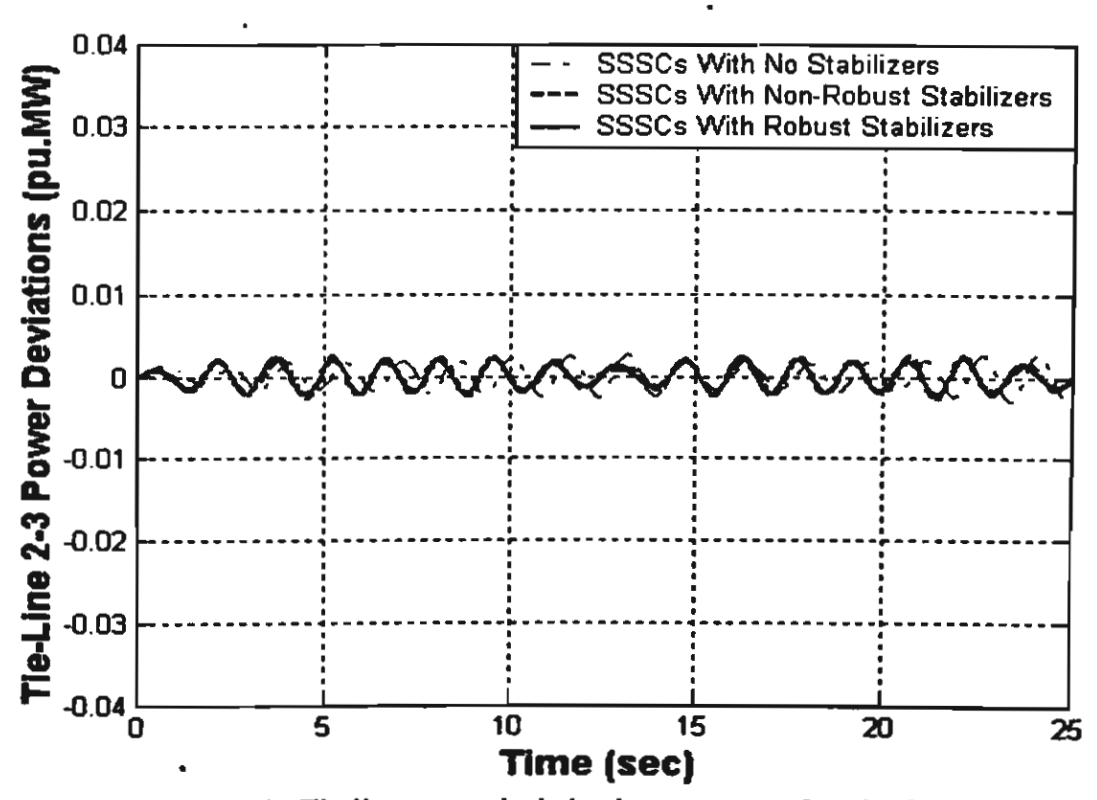


Figure 4.14: Tie-line power deviation between areas 2 and 3 for case 1

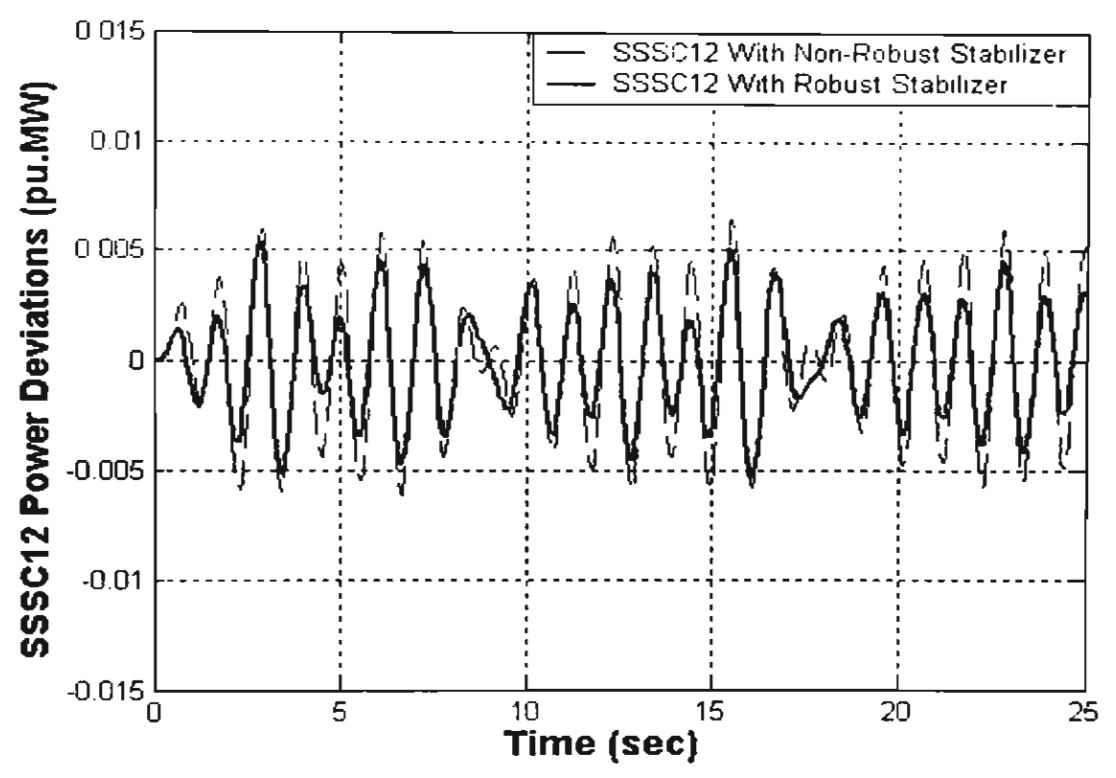


Figure 4.15: Power output deviation of SSSC12 for case 1

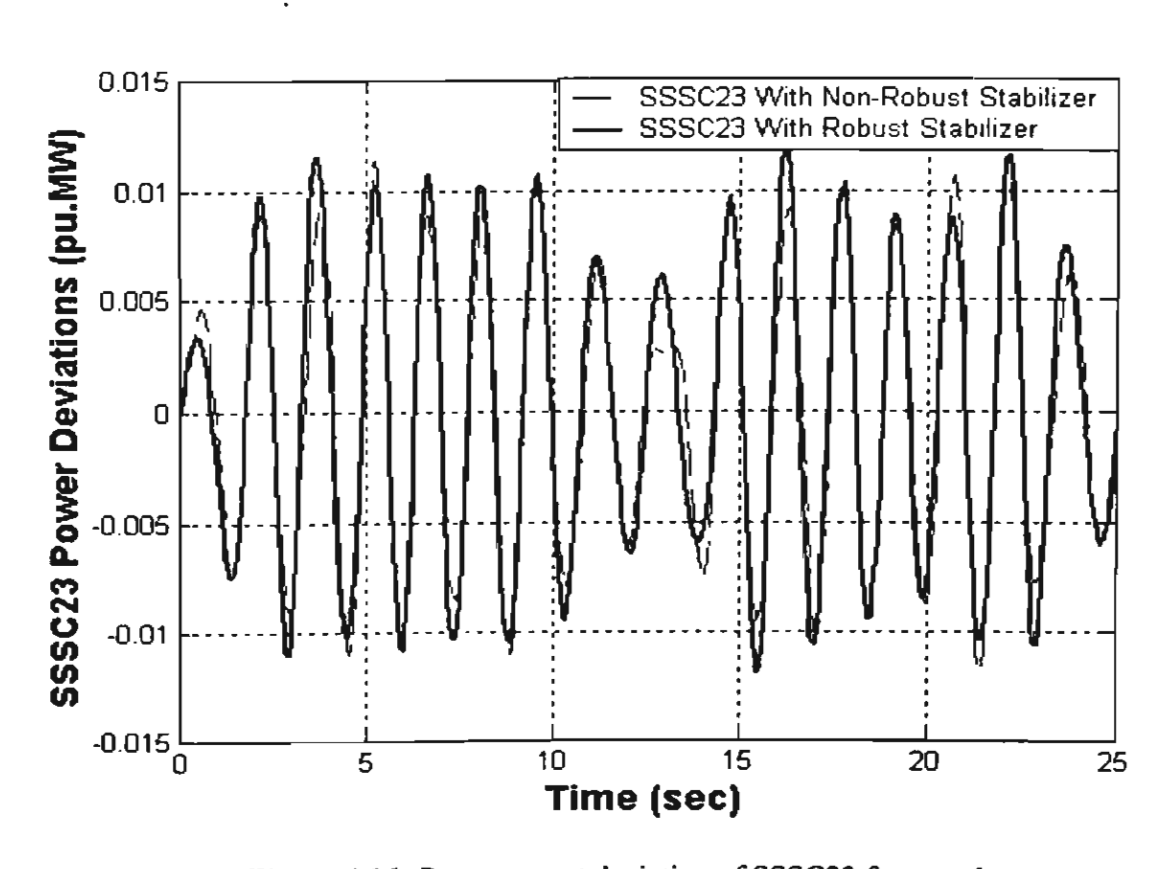


Figure 4.16: Power output deviation of SSSC23 for case 1

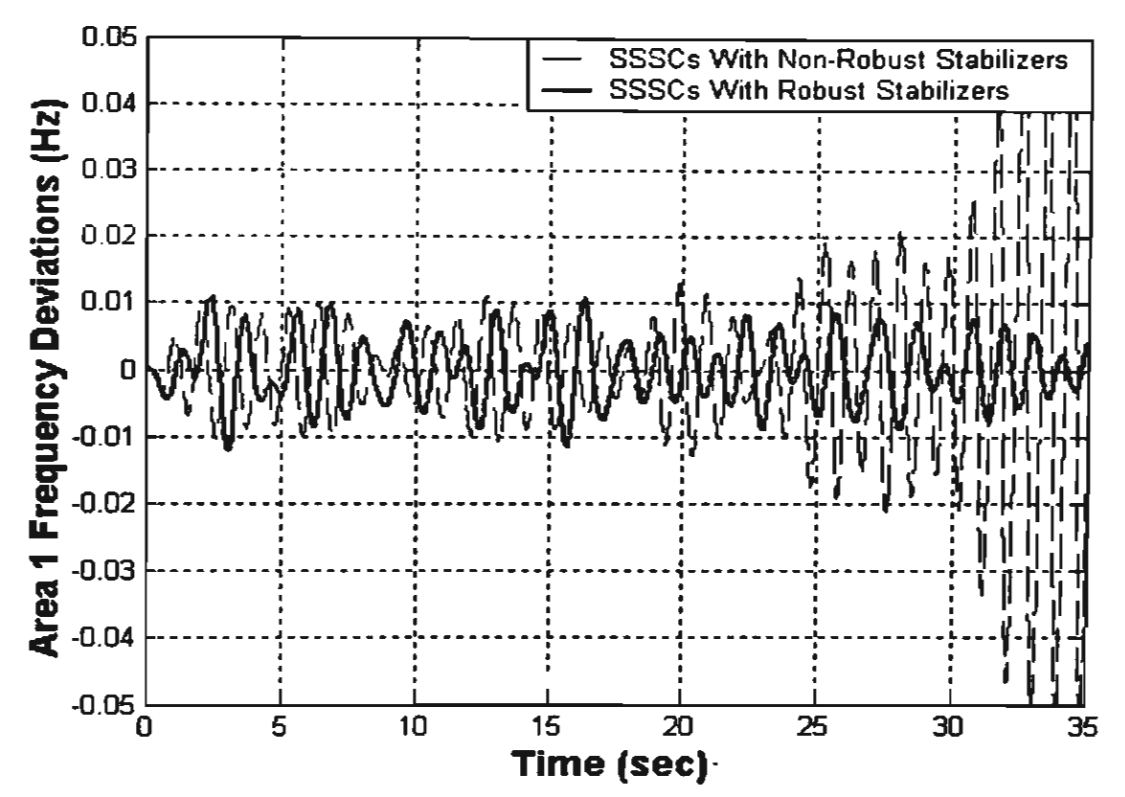


Figure 4.17: Frequency deviation of area 1 for case 2

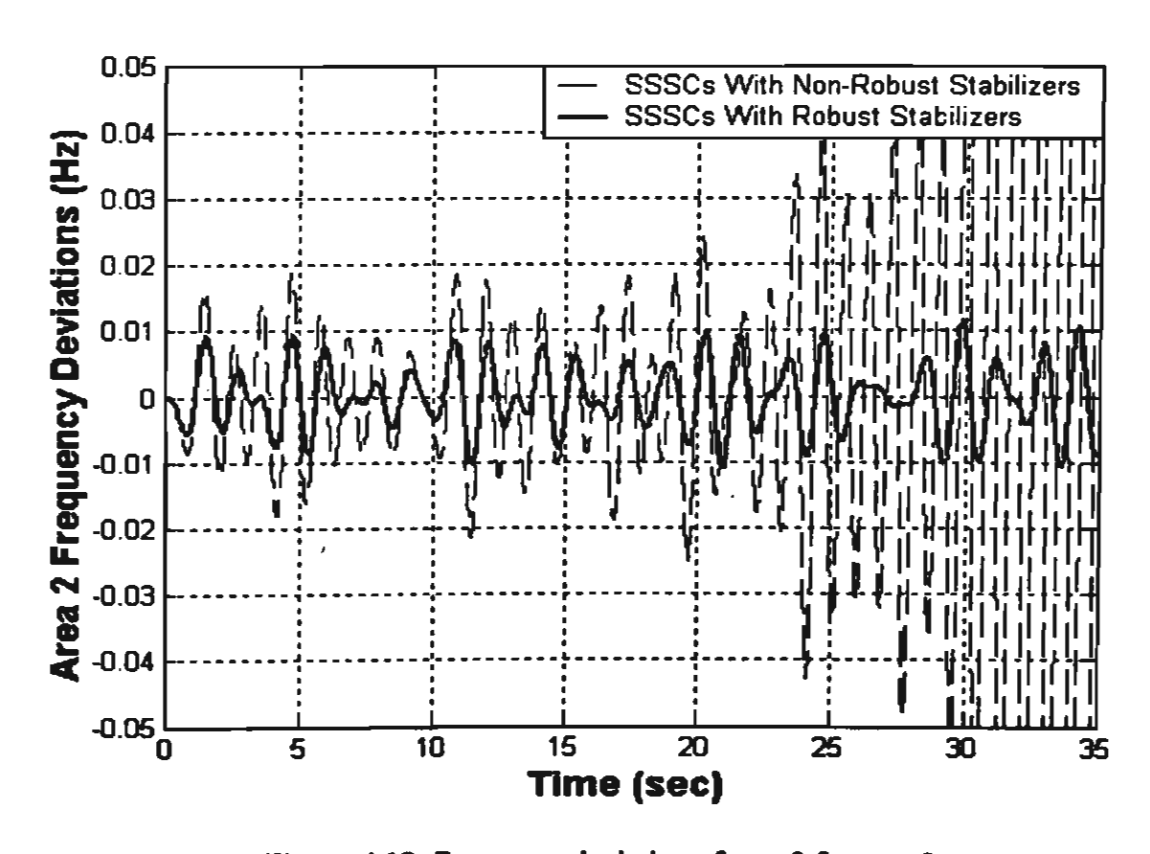


Figure 4.18: Frequency deviation of area 2 for case 2

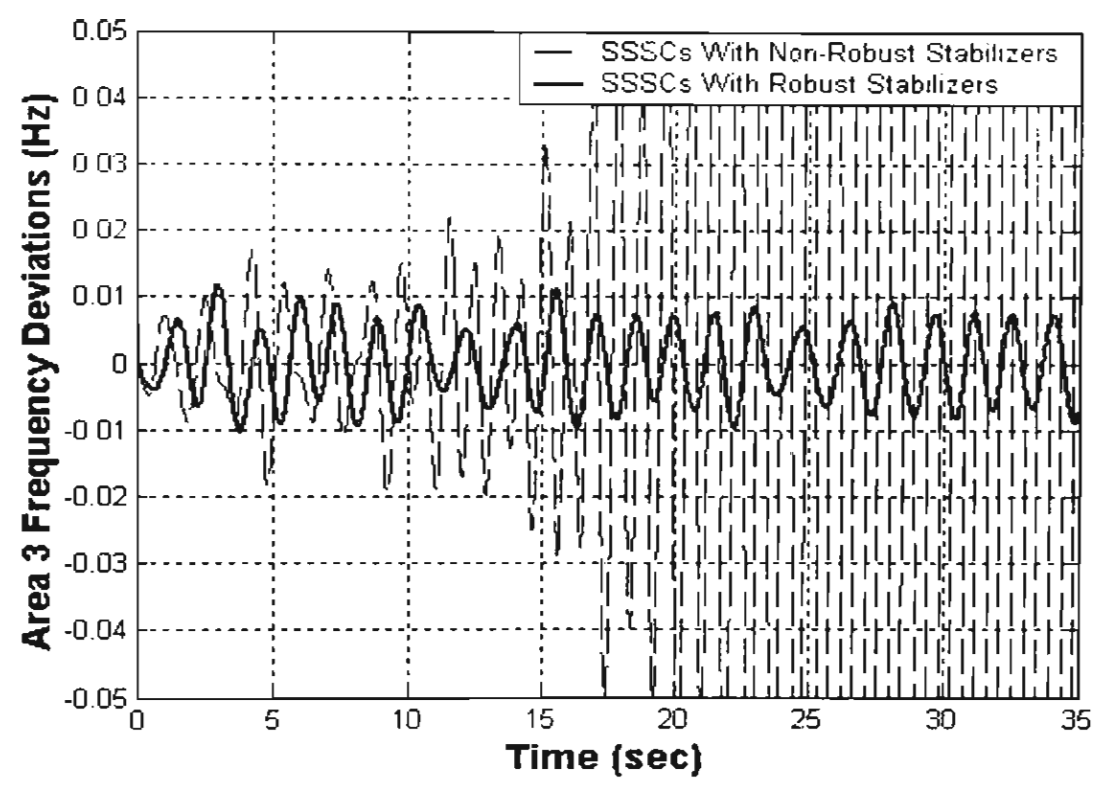


Figure 4.19: Frequency deviation of area 3 for case 2

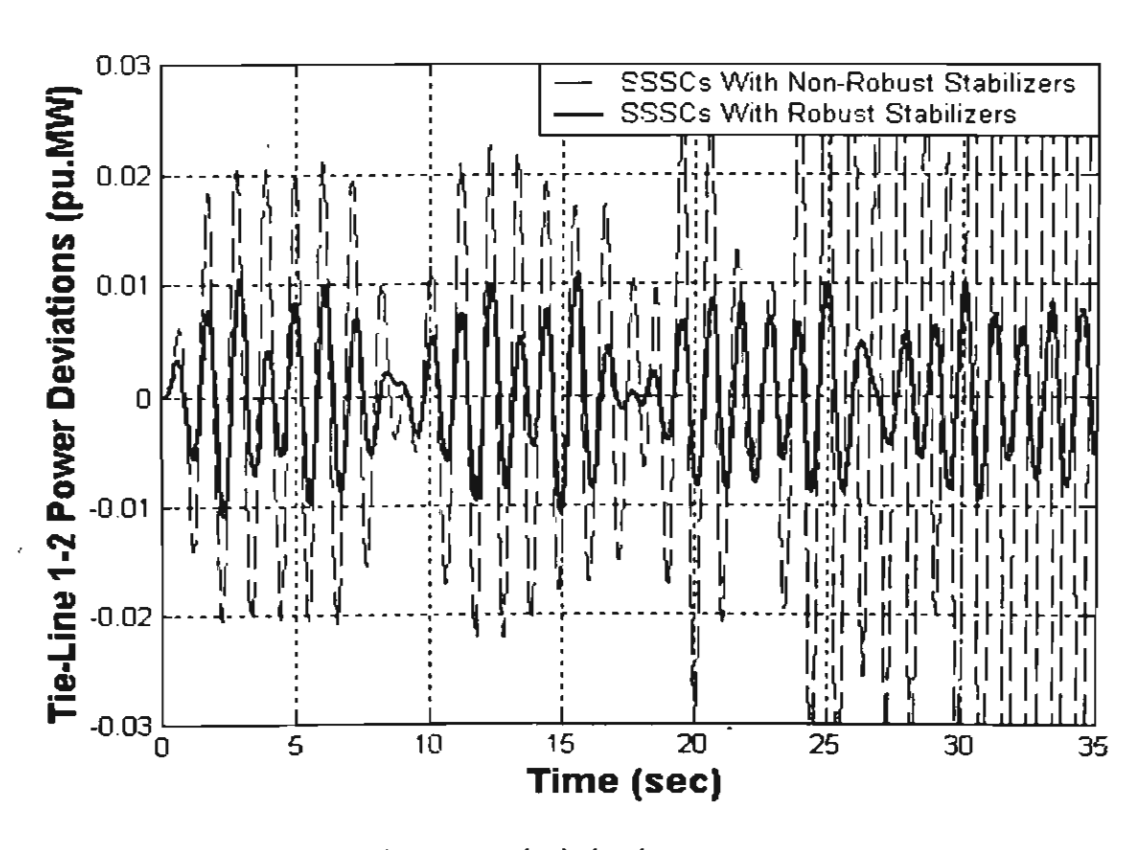


Figure 4.20: Tie-line power deviation between areas 1 and 2 for case 2

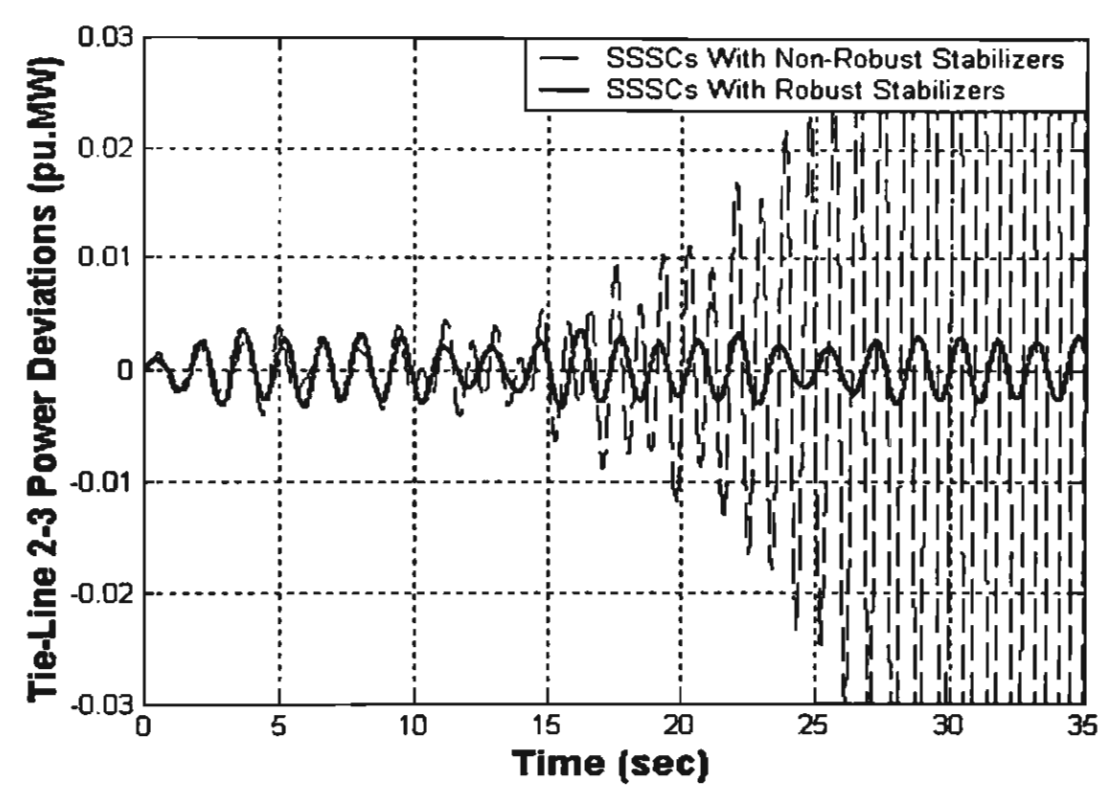


Figure 4.21: Tie-line power deviation between areas 2 and 3 for case 2

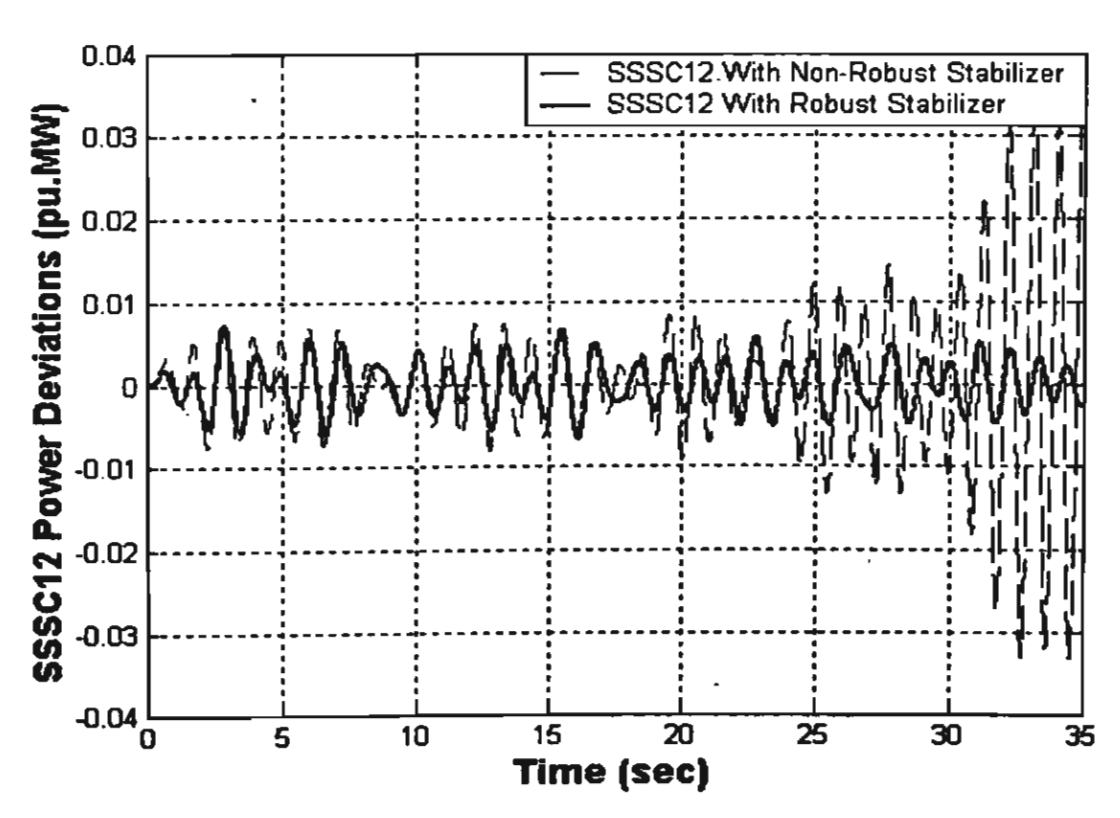


Figure 4.22: Power output deviation of SSSC12 for case 2

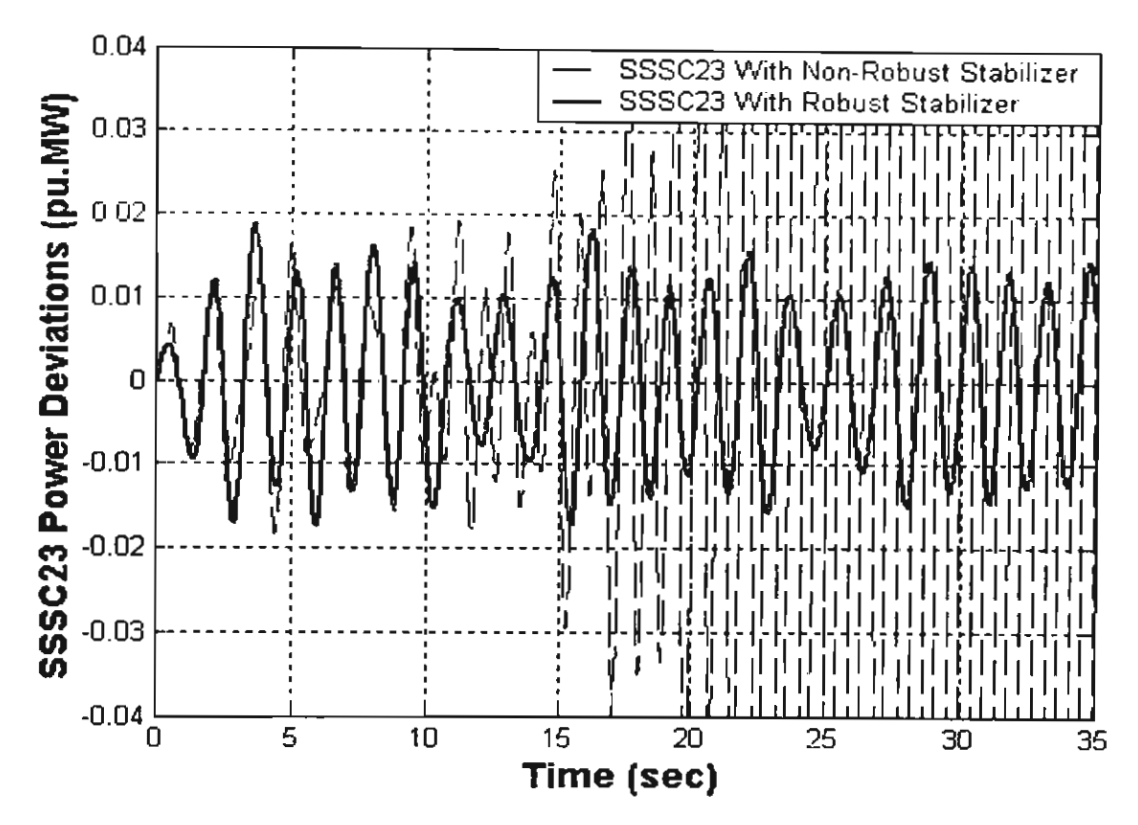


Figure 4.23: Power output deviation of SSSC23 for case 2

#### 4.5. Conclusions

This chapter focuses on the new robust design of discrete frequency stabilizer of SSSC by taking system uncertainties into account. The design method utilizes the merit of overlapping decompositions technique to extract the subsystem embedded with the inter-area oscillation mode of interest. By including the multiplicative uncertainty model in the extracted subsystem, the robust stability index based on multiplicative stability margin can be applied in the formulation of objective function. As a result, the robust stability margin of system with designed frequency stabilizer can be improved. Without trial and error, the tabu search algorithm is automatically applied to search for the optimal control parameters of the continuous-based second-order lead/lag stabilizer. As a result, the discrete-based frequency stabilizer can be easily achieved by using z-transformation of the resulted continuous-based stabilizer. The high robustness of the discrete frequency stabilizer against various load disturbances with changing frequency in the vicinity of inter-area mode and negative damping, has been confirmed by simulation study.

### Chapter 5

### Summary

In this report, a new robust design method of frequency stabilizer of SSSC has been proposed. The concept and the practical motivations for application of the proposed control have been clarified. The systematic design of SSSC frequency stabilizer in a general multi-area interconnected power system has been presented. Evaluation study has confirmed the significant effects of the frequency stabilizer designed by the proposed method.

The main outcomes from this research can be summarized as follows.

- This research proposes a new application of static synchronous series compensator (SSSC) as an apparatus to stabilization of frequency oscillations in an interconnected power system. The dynamic control of tie line power flow of SSSC located in series with tie line between interconnected areas can be applied to stabilize frequency oscillations via the system interconnections.
- The coordinated control of SSSC and governor system has been implemented.
   The SSSC plays a role in suppressing the magnitude of the transient frequency oscillation, while the governor is responsible for eliminating the steady state error of frequency oscillation.
- The SSSC is a very effective stabilization strategy of frequency oscillations for a
  system which has insufficient frequency control capability. By transferring the
  large control capability of an interconnected system via an SSSC, the problem of
  frequency oscillation in the target area can be alleviated.
- The design method utilizes the merit of overlapping decompositions technique to
  extract the subsystem embedded with the inter-area oscillation mode of interest.
  By virtue of overlapping decompositions, the physical characteristic of the power
  system can be preserved in the reduced system.
- The multiplicative uncertainty model is applied to represent all possible
  unstructured uncertainties in interconnected power systems. As a result, the
  robust stability margin against uncertainties can be easily guaranteed in terms of
  the multiplicative stability margin (MSM). Based on this uncertainty model, the
  MSM can be also incorporated in the objective function which the index of
  disturbance attenuation performance is already taken into consideration.
- The configuration of frequency stabilizer presented here is practically based on a second-order lead lag compensator with a single input signal. Without trial and error, the control parameters of the frequency stabilizer are automatically

- optimized by a tabu search algorithm, so that the desired damping ratio of the target inter-area mode and the best MSM are achieved.
- The robust frequency stabilizer can be designed based on the proposed method in continuous time domain. In addition, to implement in real power system, the continuous based frequency stabilizer can be easily transformed to the discrete based frequency stabilizer by digital control technique.
- Several simulation studies clearly show the high robustness of the frequency stabilizer under large load with changing frequency in the vicinity of the interarea oscillation mode and negative damping.

### References

- 1. F. D. Galliana and M. Illic, *Power System Restructuring*, Kluwer Academic Publishers, 1998.
- 2. L. Philipson and H. L. Willis, *Understanding Electric Utilities and De-Regulation*, Marcel Dekker, 1999.
- 3. K. N. Zadeh, R. C. Meyer and G. Cauley, Practices and new concepts in power system control, *IEEE Transactions on Power Systems*, Vol. 11, No. 1, pp. 3-9, 1996.
- 4. L. H. Fink and P. J. M. Van Son, On system control within a restructured Industry, *IEEE Transactions on Power Systems*, Vol.13, No. 2, pp. 611-616, 1998.
- Interconnected Operations Service Working Group, Defining Interconnected Operation Service Under Open Access, 1997, available at www.nerc.com
- M. Ilic and S. Liu, Hierarchical Power System Control, Its Value in a Changing Industry, Springer-Verlag, 1996.
- R. Christie and A. Bose, Load Frequency Control Issues in Power System Operations after Deregulation, *IEEE Transactions on Power Systems*, Vol. 11, No. 3, pp. 1191-1200, 1996.
- 8. B. H. Bakken and O. S. Grande, Automatic Generation Control in Deregulated Power System, *IEEE Transactions on Power Systems*, Vol. 13, No. 4, pp. 1401-1406, 1998.
- N. Jaleeli, L.S. Vanslyck, D.N. Ewart, L.H. Fink and A.G. Hoffmann, Understanding automatic generation control, *IEEE Transactions on Power Systems*, Vol. 7, No. 3, pp. 1106-1122, 1999.
- C. Concordia and L. K. Kirchmayer, Tie Line Power and Frequency Control of Electric Power Systems, Part I, II, III: AIEE Trans. Vol. 72, 1954.
- 11. O.L. Elgerd, Electric Energy System Theory, An Introduction 2nd. McGraw-Hill, 1985.
- 12. P. Kundur, Power System Stability and Control, McGraw Hill, 1994.
- 13. A. J. Wood and B.F. Wollenberg, Power Generation, Operation and Control, 2<sup>nd</sup> Edition, John Wiley & Sons, 1996.
- 14. Yao Nan Yu, Electric Power System Dynamics, Academic Press, 1983.
- J. Machowski, J. W. Bialek and J. R. Bumby, Power System Dynamics and Stability, John Wiley & Sons, 1997.
- N. G. Hingorani, High Power Electronics and Flexible AC Transmission Systems, IEEE Power Engineering Review, pp. 3-4, 1988.
- 17. IEEE FACTS Working Group and GIGRE FACTS Working Group, FACTS Overview, IEEE 95 TP 108, 1995.
- 18. IEEE Power Engineering Society, FACTS Applications, IEEE 96 TP 116-0, 1996.

- 19. N. G. Hingorani and L. Gyugyi, Understanding FACTS: Concepts and Technology of Flexible AC Transmission Systems, IEEE PRESS, 2000.
- 20. L. Gyugyi, Dynamic compensator of AC transmission lines by solid-state synchronous voltage source, *IEEE Transactions on Power Delivery*, Vol. 9, No. 2, pp. 904-911, 1994.
- 21. L. Gyugyi, C. D. Schauder and K.K. Sen, Static Synchronous Series Compensator: A Solid-State Approach to The Series Compensation of Transmission Lines, *IEEE Transactions on Power Delivery*, Vol. 12, No. 1, pp. 406-417, 1997.
- 22. N. G. Hingorani, Power Electronics in Electric Utilities: Role of Power Electronics in Future Power Systems, *Proceedings of IEEE*, Vol. 76, No. 4, pp. 481-482, 1988.
- 23. L. Gyugyi, Unified Power Flow Control Concept for Flexible AC Transmission Systems, *IEE Proceedings, Part C*, Vol. 139, No. 4, pp. 323-331, 1992.
- 24. A. A. Edris, Enhancement of First Swing Stability Using A High Speed Phase Shifter, *IEEE Transactions on Power Systems*, Vol. 6, No. 3, pp. 1113-1118, 1991.
- 25. M. Noroozian, L. Anguist, M. Chandhari and G. Anderesson, Improving Power System Dynamics by Series-Connected FACTS Devices, *IEEE Transactions on Power Delivery*, Vol. 12, No. 4, pp. 1635-1641, 1997.
- 26. G. El-Saady, A Variable Structure Static Phase Shifting Transformer for Power System Stabilization, *Electric Power System Research*, Vol. 50, pp. 71-78, 1999.
- 27. H. Fujita, H. Kurebayashi, H. Nohara, M. Goto and Y. Kito, Loop Power System Control by High Speed Phase Shifter, *Transactions of IEE of Japan*, Vol. 114-B, No. 5, pp. 475-482, 1994.
- 28. K. Xing and G. L. Kusic, Damping Subsynchronous Resonance by Phase Shifters, *IEEE Transactions on Energy Conversions*, Vol. 4, No. 3, pp. 344-350, 1989.
- 29. K. K. Sen, SSSC Static Synchronous Series Compensator, Theory, Modeling and Applications, *IEEE Transactions on Power Delivery*, Vol. 13, No. 1, pp. 241-246, 1998.
- 30. Y. Morioka, M. Kato, Y. Mishima, Y. Nakachi, M. Asada and K. Tokuhara, Implementation of Unified Power Flow Controller and Verification for Transmission Capability Improvement, *IEEE Transactions on Power Systems*, Vol. 14, No. 2, pp. 575-581, 1999.
- 31. B. A. Renz, A. J. F. Keri, A. S. Mehraban, J. P. Kessinger, C. D. Schauder, L. Gyugyi, L. J. Kovalskym, A. Edris, World's First Unified Power Flow Controller on the AEP System, *CIGRE*, Session 1998, Paper 14-107.
- 32. M. Ikeda, D.D. Siljak and D. E. White, Decentralized control with overlapping information sets. *Journal of Optimization Theory and Applications*, Vol. 34, No. 2, pp.279-310, 1981.
- 33. B. Shahian and M. Hassul, Control System Design using MATLAB, Prentice Hall, 1993.

- 34. S. Skogestad and I. Postlethwaite, Multivariable Feedback Control, Analysis and Design, John Wiley & Sons, 1998.
- 35. G. C. Goodwin, S. F. Graebe and M. E. Salgado, *Control System Design*, Prentice Hall, 2001.
- 36. F. Glover and M. Laguna, Tabu Search. Kluwer Academic Publishers. 2000.
- 37. V. J. Rayward-Smith, I. H. Osman, C.R. Reeves, and G.D. Smith, *Modern Heuristic Search Methods*, John Wiley & Sons, UK, 1996.

## **List of Publications**

- 1. Issarachai Ngamroo and Waree Kongprawechnon: A robust controller design of SSSC for stabilization of frequency oscillations in interconnected power systems, *Electric Power System Research*, 2003. (Article in press)
- 2. Issarachai Ngamroo and Waree Kongprawechnon: Robust frequency stabilizer design of SSSC taking into consideration system uncertainties, Submitted to ASEAN Journal on Science & Technology for Development

## ARTICLE IN PRESS



Available online at www.sciencedirect.com

ELECTRIC POWER SYSTEMS RESEARCH

Electric Power Systems Research xxx (2003) xxx-xxx

www.elsevier.com/locate/epsi

# A robust controller design of SSSC for stabilization of frequency oscillations in interconnected power systems

I. Ngamroo\*, W. Kongprawechnon

Electrical Power Engineering Program, Sirindhorn International Institute of Technology, Thammasat University, Pathwothani 12121, Thailand

Received 22 July 2002; received in revised form 19 March 2003; accepted 23 March 2003

#### Abstract

10

11

12

13

14

15

16

17

18

19

20

21 22

24

26

27

28

29

30

31

32

33

34

35

36

37

39

40

41

As an AC interconnected power system is subjected to a large load with rapid change, system frequency may be severely disturbed and becomes oscillatory. To stabilize the frequency oscillations, the dynamic power flow control of the Static Synchronous Series Compensator (SSSC) located in series with the tie line between interconnected power systems, is employed. By regarding the system interconnection as the control channel, the power flow control by an SSSC via the interconnection creates a sophisticated method of frequency stabilization. To implement this concept, the robust design method of the lead/lag controller equipped with the SSNC is proposed. In the design process, not only the attenuation performance of system disturbances, but also the robust stability against system uncertainties are taken into consideration. The optimal parameters of the lead/lag controller are obtained by using the tabu search algorithm (TSA), so that both performance and robustness are satisfied. In addition, the technique of overlapping decompositions is applied to reduce the order of the study power system, meanwhile the physical characteristic is still preserved. Simulation study exhibits the significant effect of designed controller on the study four-area interconnected power system under different load disturbances and variation of system parameters.

23 (b) 2003 Published by Elsevier B.V.

Keywords FACTS; SSSC: Robust control: Tabu search algorithm: Overlapping decompositions; Power system stabilization; Frequency oscillations;

25 Ancillary services

#### 1. Introduction

Nowadays, the electric power system is in transition to a fully competitive deregulated scenario. Under this circumstance, any power system controls such as frequency and voltage controls will be served as ancillary services [1.2]. Especially, in the case that the proliferation of non-utility generations, i.e. Independent Power Producers (IPPs) that do not possess sufficient frequency control capabilities, tends to increase considerably. Furthermore, various kinds of apparatus with large capacity and fast power consumption such as a magnetic levitation transportation, a testing plant for nuclear fusion, or even an ordinary scale factory like a steel manufacturer etc. increase significantly. When these loads are concentrated in a power system, they may cause a serious problem of frequency oscillations.

Under this situation, the conventional frequency control, i.e. governor, may no longer be able to absorb the large frequency oscillations due to its slow response [3]. A new service of stabilization of frequency oscillations becomes challenging and is highly expected in the future competitive environment.

45

46

49

59

To tackle this problem, the authors have proposed a new stabilization of frequency oscillations by the Static Synchronous Series Compensator (SSSC) [4]. The SSSC is a Flexible AC Transmission Systems (FACTS) device, that has been highly expected as an effective apparatus with an ability of dynamic power flow control [5]. In [4], the SSSC is located in series with the tie line between two-area interconnected power system. By regarding the system interconnection as the channel of power flow control by SSSC, the system frequency oscillations under a sudden load disturbance can be stabilized effectively. However, the proposed control scheme of SSSC in [4] is designed based on a state feedback scheme

<sup>\*</sup>Corresponding author Tel +66-2986-9009, fax: +66-2986-9112. E-mail address: ngamroo@siit tu.ac th (Issarachai Ngamroo)

<sup>0378-7796/03/5 ,</sup> see front matter  $|\psi|$  2003 Published by Elsevier B V doi 10 1016/S0378-7796(03)00110-X

8n

of variables. Therefore, it is not easy to implement in a multi-area interconnected power system.

In this paper, the new control design of SSSC is presented. The lead/lag controller with a single feedback signal input is equipped with an SSSC. To determine the optimal parameters of the lead/lag controller, the tabu search algorithm (TSA) [6] is employed. TSA is a metaheuristic method that is based on a local search approach with the ability to escape from being trapped in local optima. It has been applied to solve many problems of power system optimization [7-11]. In the formulation of the objective function, not only the attenuation of system disturbances, but also the robust stability of controller against system uncertainties are taken into consideration. In addition, the technique of overlapping decompositions is applied to reduce the order of the study power system for simplicity of control design.

The organization of this paper is as follows. First, the motivation of the proposed control of SSSC is provided. Next part deals with the design methodology including the coordinated control of SSSC and governors, the mathematical model of SSSC, the system reduction by overlapping decompositions, the objective function formulation, and the TSA. Subsequently, the evaluation of the proposed controller in a four-area interconnected power system is outlined by simulation study. Lastly, a conclusion is given.

#### 2. Motivation of proposed frequency stabilization

Fig. 1 shows the four-area interconnected power system with a loop configuration. This system is used to explain the motivation of the proposed control design. It is assumed that a large load with rapid change has been installed in an area 1. This load change causes serious frequency oscillations. Moreover, IPPs that do not possess frequency control capabilities are included

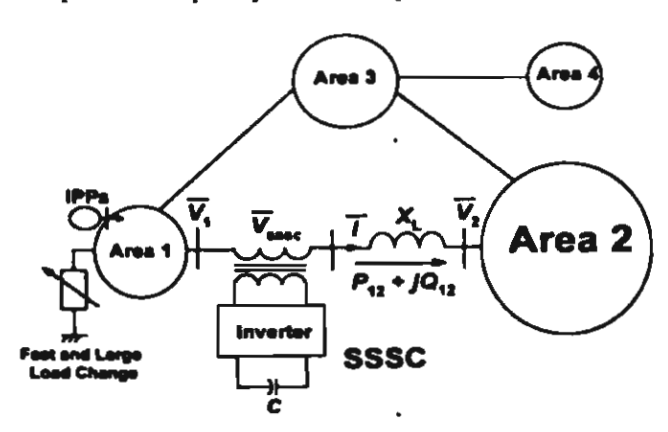


Fig. 1. An SSSC in a four-area interconnected power system.

in an area 1. Under this situation, the governors in an area I can not sufficiently provide adequate frequency control. On the contrary, the area 2 has large control capability enough to spare for other areas. Therefore, an area 2 offers a service of frequency stabilization to an area 1 by using the SSSC. Since SSSC is a seriesconnected device, the power flow control effect is independent of an installed location. In the proposed design method, the SSSC controller uses the frequency deviation of area 1 as a local signal input. Therefore, the SSSC is placed at the point near an area 1. Note that the SSSC is utilized as the energy transfer device from area 2 to area 1. As the frequency fluctuation in an area 1 occurs, the SSSC will provide the dynamic control of a tie line power via the system connections. By exploiting the system interconnections as the control channels, the frequency oscillations can be stabilized.

#### 3. Design of SSSC controller

#### 3.1. Coordinated control of SSSC and governors

The performance of SSSC is extremely rapid when compared with the conventional frequency control system, i.e. governor. The difference in the performance signifies that SSSC and governors may be coordinated as follows. When an area is subjected to a sudden load disturbance, the SSSC quickly acts to minimize the peak value of the frequency deviation. Subsequently, the governors are responsible for eliminating the steady-state errors of frequency deviations. Based on this concept, the periods of operation for two devices do not overlap. Consequently, the dynamics of the governors can then be neglected in the control design of the SSSC for the sake of simplicity.

#### 3.2. Mathematical model of the SSSC

In this study, the mathematical model of the SSSC for stabilization of frequency oscillations is derived from the characteristic of power flow control by SSSC [5]. By adjusting the output voltage of SSSC ( $\bar{V}_{SSSC}$ ), the tie line power flow ( $P_{12} + jQ_{12}$ ), can be directly controlled as shown in Fig. 1. Since the SSSC fundamentally controls only the reactive power, then the phasor  $\bar{V}_{SSSC}$  is perpendicular to the phasor of line current  $\bar{I}$ , which can be expressed as

$$\tilde{V}_{SSSC} = jV_{SSSC}\tilde{I}/I \tag{1}$$

where  $V_{\rm SSSC}$  and I are the magnitudes of  $\bar{V}_{\rm SSSC}$  and  $\bar{I}$ , respectively. Note that,  $\bar{I}/I$  is a unit vector of line current. Therefore, the current  $\bar{I}$  in Fig. 1, can be expressed as

I. Ngamroo, W. Kongprawechnon I Electric Power Systems Research xxx (2003) xxx-xxx

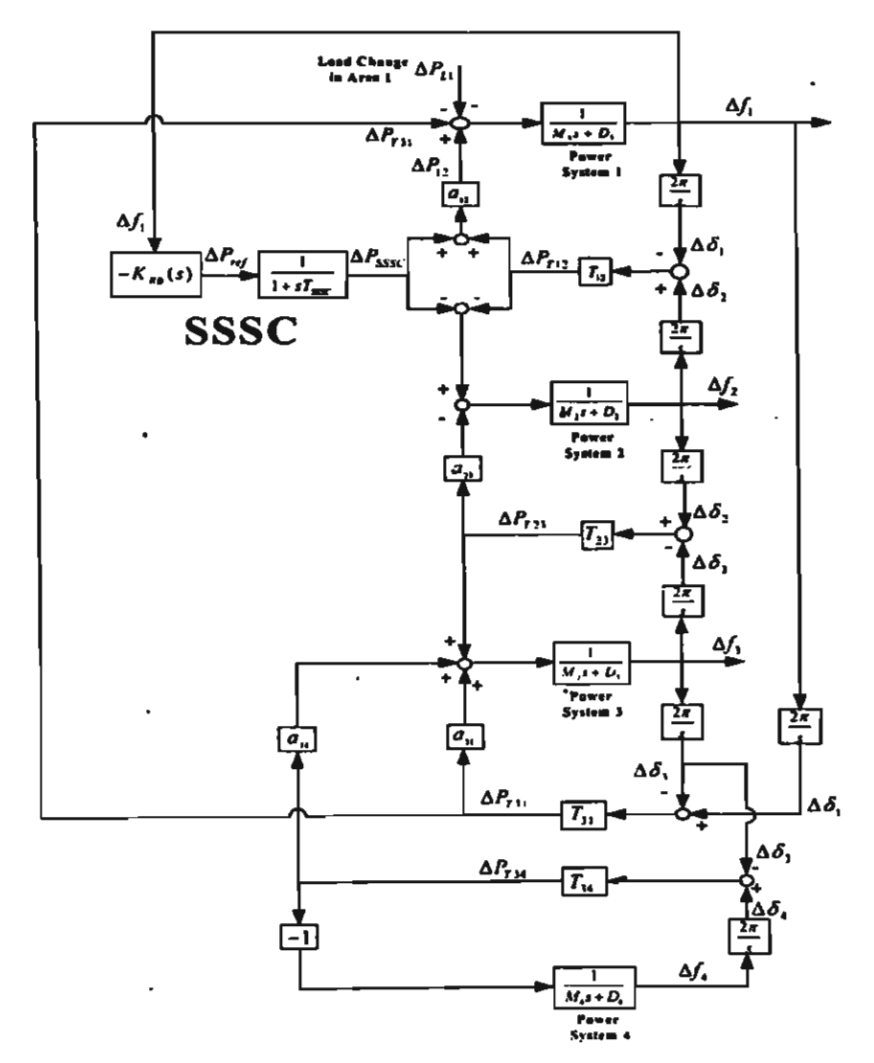


Fig. 2. An SSSC in a linearized four-area interconnected power system without governors.

143 
$$\bar{I} = \frac{\bar{V}_1 - \bar{V}_2 - jV_{\text{SSSC}}\bar{I}/I}{jX_L}$$
 (2)

where  $X_L$  is the reactance of a tie line,  $\bar{V}_1$  and  $\bar{V}_2$  are the voltages at buses 1 and 2, respectively. The active power

145 and reactive power flow through bus 1 are

146 
$$P_{12} + jQ_{12} = \bar{V}_1 \tilde{I}^*$$
 (3)

where  $\bar{I}^*$  is a conjugate of  $\bar{I}$ . Substituting  $\bar{I}$  from (2) into

147 (3) yields

148 
$$P_{12} + jQ_{12} = \frac{V_1 V_2}{X_L} \sin(\delta_1 - \delta_2) - V_{\text{SSSC}} \frac{\bar{V}_1 \bar{I}^*}{X_L \bar{I}} + j \left( \frac{V_1^2}{X_L} - \frac{V_1 V_2}{X_L} \cos(\delta_1 - \delta_2) \right). \tag{4}$$

where  $\bar{V}_1 = V_1 e^{j\delta 1}$  and  $\bar{V}_2 = V_2 e^{j\delta_2}$ . In the second term of the right hand side of (4),  $\bar{V}_1 \bar{I}^*$  is equal to  $P_{12} + jQ_{12}$ 

(see (3)). Accordingly, the relation in the real part of (4) provides 151

 $P_{12} = \frac{V_1 V_2}{X_I} \sin(\delta_1 - \delta_2) - \frac{P_{12}}{X_I I} V_{SSSC}$  (5) 152

153

154

155

156

$$F_{12} = \frac{1}{X_I} \sin(\theta_1 - \theta_2) - \frac{1}{X_I I} v_{SSSC}$$
 (5) 152

In (5), the second term of the right hand side is the active power controlled by SSSC. Here, it is assumed that  $V_1$  and  $V_2$  are constant and the initial value of  $V_{\rm SSSC}$  is zero, i.e.  $V_{\rm SSSC0} = 0$ . By linearizing (5) about an initial operating point,

$$\Delta P_{12} = \frac{V_1 V_2 \cos(\delta_{10} - \delta_{20})}{X_I} (\Delta \delta_1 - \Delta \delta_2) - \frac{P_{120}}{X_I I_0} \Delta V_{SSSC}$$
 157

where the subscript "0" denotes the value at the initial operating point. As the voltage deviation of SSSC 158

1. Ngamroo, W. Kongprawechnon I Electric Power Systems Research xxx (2003) xxx-xxx

 $(\Delta V_{\rm SSSC})$  is adjusted, the power output deviation injected by SSSC can be controlled as  $\Delta P_{\rm SSSC} = -(P_{120}/X_II_0)\Delta V_{\rm SSSC}$ . Equation (6), therefore, implies that the SSSC is capable of controlling the active power independently. Here, the SSSC is represented by the active power controller. The control effect by SSSC is expressed by the injected power deviation  $\Delta P_{\rm SSSC}$  instead of  $-(P_{120}/X_II_0)\Delta V_{\rm SSSC}$ . As a result, (6) can be expressed as

$$\Delta P_{12} = \Delta P_{T12} + \Delta P_{SSSC} \tag{7}$$

where

$$\Delta P_{T12} = \frac{V_1 V_2 \cos(\delta_{10} - \delta_{20})}{X_t} (\Delta \delta_1 - \Delta \delta_2)$$

$$= T_{12} (\Delta \delta_1 - \Delta \delta_2)$$
 (8)

and  $T_{12}$  is a synchronizing power coefficient.

### 3.3. Design methodology

A study system depicted in Fig. 1 is used to explain the proposed control design of SSSC. The linearized four-area interconnected system [12] including the active power model of SSSC is delineated in Fig. 2.

Based on the coordinated control of SSSC and governors, the dynamics of governors are eliminated in this figure. The active power controller of SSSC has a structure of the lead/lag compensator  $K_{RB}(s)$  with output signal  $\Delta P_{ref}$ . In this study, the dynamic characteristic of SSSC is modeled as the first order controller with time constant  $T_{\rm SSSC}$ . Note that the injected power deviation of SSSC,  $\Delta P_{\rm SSSC}$  acting positively on the area 1 reacts negatively on the area 2. Therefore,  $\Delta P_{\rm SSSC}$  flows into both areas with different signs (+, -), simultaneously. This characteristic represents the physical meaning of (7). The linearized system in Fig. 2 can be expressed as

where,  $\Delta f_i$  is the frequency deviation of area i,  $\Delta P_{Tij}$  is the tie line power deviation between areas i and j,  $M_i$  is the inertia constant of area i,  $D_i$  is the damping coefficient of area i,  $a_{ij}$  is the area capacity ratio between areas i and j,  $T_{ij}$  is the synchronizing power coefficient of the tie line between areas i and j, where i,  $j=1,\ldots,4$ . Here  $a_{S12}=(a_{12}+T_{31}/T_{12})/M_1$ ,  $a_{S14}=-T_{31}/(M_1T_{23})$ ,  $a_{S52}=-a_{31}T_{31}/(M_3T_{12})$ ,  $a_{S54}=(1+a_{31}T_{31}/T_{23})/M_3$ . The variable  $\Delta P_{T31}$  is represented in terms of  $\Delta P_{T12}$  and  $\Delta P_{T23}$  by

$$\Delta P_{T31} = -\frac{T_{31}}{T_{12}} \Delta P_{T12} + \frac{T_{31}}{T_{23}} \Delta P_{T23}$$
 (10) 198

Thus,  $\Delta P_{T31}$  has disappeared in (9). This system has three conjugate pairs of complex eigenvalues and a negative real eigenvalue. The former corresponds to three inter-area oscillation modes, and the latter the inertia center mode. In this paper, the design purpose of SSSC is to enhance the damping of the inter-area mode between areas 1 and 2. The proposed design can be divided into three steps as follows.

## 3.3.1. Reduction of power system model by overlapping decompositions [13]

The concept of overlapping decompositions is applied to the system (9) with the aim of extracting the subsystem where the inter-area mode between areas 1 and 2 is preserved. The system (9) is referred to as the system S. The state variables of S are classified into three groups, i.e.  $x_1 = [\Delta f_1]$ ,  $x_2 = [\Delta P_{T12}]$ ,  $x_3 = [\Delta f_2, \Delta P_{T23}, \Delta f_3, \Delta P_{T34}, \Delta f_4]^T$ . Therefore, the system S can be expressed in compact form as

$$S: \begin{bmatrix} \dot{x}_1 \\ \dot{x}_2 \\ \dot{x}_3 \end{bmatrix} = \begin{bmatrix} A_{11} & A_{12} & A_{13} \\ A_{21} & A_{22} & A_{23} \\ A_{31} & A_{32} & A_{33} \end{bmatrix} \begin{bmatrix} x_1 \\ x_2 \\ x_3 \end{bmatrix} + \begin{bmatrix} B_{11} \\ B_{21} \\ B_{31} \end{bmatrix} \Delta P_{SSSC} \quad (11) \quad 216$$

The sub-matrices  $A_{ij}$  and  $B_{i1}$ , (i, j = 1, 2, 3) have

$$S: \begin{bmatrix} \Delta f_1 \\ \Delta \dot{P}_{12} \\ \Delta \dot{P}_{22} \\ \Delta \dot{P}_{34} \\ \Delta \dot{f}_4 \end{bmatrix} = \begin{bmatrix} -D_1 & a_{s12} & 0 & a_{s14} & 0 & 0 & 0 \\ -2\pi T_{12} & 0 & 2\pi T_{12} & 0 & 0 & 0 & 0 \\ 0 & -\frac{1}{M_2} & -\frac{D_2}{M_2} & -\frac{a_{21}}{M_2} & 0 & 0 & 0 \\ 0 & 0 & 2\pi T_{23} & 0 & -2\pi T_{23} & 0 & 0 \\ 0 & a_{s52} & 0 & a_{s54} & -\frac{D_3}{M_3} & \frac{a_{34}}{M_3} & 0 \\ 0 & 0 & 0 & 0 & 0 & -2\pi T_{34} & 0 & 2\pi T_{34} \\ 0 & 0 & 0 & 0 & 0 & -2\pi T_{34} & 0 & 2\pi T_{34} \\ 0 & 0 & 0 & 0 & 0 & -\frac{1}{M_4} & -\frac{D_4}{M_4} \end{bmatrix} \begin{bmatrix} \Delta f_1 \\ \Delta P_{712} \\ \Delta f_2 \\ \Delta P_{723} \\ \Delta f_3 \\ \Delta P_{734} \\ \Delta f_4 \end{bmatrix} + \begin{bmatrix} a_{12} \\ M_1 \\ 0 \\ 1 \\ M_2 \\ 0 \\ 0 \\ 0 \\ 0 \\ 0 \end{bmatrix} \Delta P_{SSSC}$$
 (9)

appropriate dimensions identical to the corresponding state and input vectors. According to the process of overlapping decompositions, the system S can be expanded as

221 
$$\tilde{S}:\begin{bmatrix} \dot{z}_1 \\ \dot{z}_2 \end{bmatrix} = \begin{bmatrix} A_{11} & A_{12} & 0 & A_{13} \\ A_{21} & A_{22} & 0 & A_{23} \\ A_{21} & 0 & A_{22} & A_{23} \\ A_{31} & 0 & A_{32} & A_{33} \end{bmatrix} \begin{bmatrix} z_1 \\ z_2 \end{bmatrix} + \begin{bmatrix} B_{11} \\ B_{21} \\ B_{21} \\ B_{31} \end{bmatrix} \Delta P_{SSSC}$$
(12)

 $z_1 = [x_1^T, x_2^T]$  and  $z_2 = [x_2^T, x_3^T]^T$ . The system  $\tilde{S}$  in (12) can be decomposed into two interconnected overlapping subsystems.

224 
$$\tilde{S}_{1}:\dot{z}_{1} = \left(\begin{bmatrix} A_{11} & A_{12} \\ A_{21} & A_{22} \end{bmatrix} z_{1} + \begin{bmatrix} B_{11} \\ B_{21} \end{bmatrix} \Delta P_{SSSC} \right) + \begin{bmatrix} 0 & A_{13} \\ 0 & A_{23} \end{bmatrix} z_{2}$$

$$(13)$$

225 
$$\vec{S}_{2}:\vec{z}_{2} = \left(\begin{bmatrix} A_{22} & A_{23} \\ A_{32} & A_{33} \end{bmatrix} z_{2}\right) + \begin{bmatrix} A_{21} & 0 \\ A_{31} & 0 \end{bmatrix} z_{1} + \begin{bmatrix} B_{21} \\ B_{31} \end{bmatrix} \Delta P_{SSSC}$$
(14)

The state variable  $x_2$ , i.e. the tie line power deviation between areas 1 and 2 ( $\Delta P_{T12}$ ), is repeatedly included in both subsystems, which implies "Overlapping Decompositions".

For system stabilization, consider two interconnected subsystems  $S_1$  and  $S_2$ . The terms in the right hand sides of (13) and (14) can be separated into the decoupled subsystems (as indicated in the parenthesis in (13) and (14)) and the interconnection subsystems. As mentioned in [13], if each decoupled subsystem can be stabilized by its own input, the asymptotic stability of the interconnected overlapping subsystems  $S_1$  and  $S_2$  are maintained. Moreover, the asymptotic stability of the original system S is also guaranteed. Consequently, the interactions of the decoupled subsystems with the interconnection subsystems in (13) and (14) are regarded as perturbations. They can be neglected during control design. As a result, the decoupled subsystems of  $S_1$  and  $S_2$  can be expressed as

244 
$$\vec{S}_{D1}:\vec{z}_1 = \begin{bmatrix} A_{11} & A_{12} \\ A_{21} & A_{22} \end{bmatrix} z_1 + \begin{bmatrix} B_{11} \\ B_{21} \end{bmatrix} \Delta P_{SSSC}$$
 (15)

245 
$$\vec{S}_{D2}:\vec{z}_2 = \begin{bmatrix} A_{22} & A_{23} \\ A_{32} & A_{33} \end{bmatrix} z_2 + \begin{bmatrix} B_{11} \\ B_{21} \end{bmatrix} \Delta P_{SSSC}$$
 (16)

In (15) and (16), there is a control input  $\Delta P_{\rm SSSC}$ 246 appearing only in the subsystem  $\vec{S}_{D1}$ . Here, the de-247 coupled subsystem  $\vec{S}_{D1}$  is regarded as the designed 248 system, which can be expressed as

$$\tilde{G}: \begin{bmatrix} \Delta f_1 \\ \Delta \dot{P}_{T12} \end{bmatrix} = \begin{bmatrix} -D_1/M_1 & a_{S12} \\ -2\pi T_{12} & 0 \end{bmatrix} \begin{bmatrix} \Delta f_1 \\ \Delta P_{T12} \end{bmatrix} + \begin{bmatrix} a_{12}/M_1 \\ 0 \end{bmatrix} \Delta P_{SSSC}$$
(17)

It can be verified that the eigenvalues of (17) are complex conjugate and are assumed to be  $-\sigma \pm j\omega_d$ . These complex eigenvalues correspond to the inter-area oscillation mode between areas 1 and 2 in the original system S. By virtue of overlapping decompositions, the physical characteristic of the original system S is still preserved after the process of system reduction. This explicitly shows the merit of overlapping decompositions.

By incorporating the dynamic characteristic of the SSSC, (17) becomes

$$G: \begin{bmatrix} \Delta f_{1} \\ \Delta \dot{P}_{T12} \\ \Delta \dot{P}_{SSSC} \end{bmatrix}$$

$$= \begin{bmatrix} -D_{1}/M_{1} & a_{S12} & a_{S12}/M_{1} \\ -2\pi T_{12} & 0 & 0 \\ 0 & 0 & -1/T_{SSSC} \end{bmatrix} \begin{bmatrix} \Delta f_{1} \\ \Delta P_{T12} \\ \Delta P_{SSSC} \end{bmatrix}$$

$$+ \begin{bmatrix} 0 \\ 0 \\ 1/T_{SSSC} \end{bmatrix} \Delta P_{ref}$$
(18)

For the input signal of SSSC controller, two available local signals, i.e. area 1 frequency deviation  $(\Delta f_1)$  and the tie line 1-2 power deviation  $(\Delta P_{T12})$  are taken into consideration. By calculating the right eigenvector of the oscillation mode between areas 1 and 2, the degree of activity [14] of  $\Delta f_1$  and  $\Delta P_{T12}$  in this mode can be evaluated. From (18), the eigenvalues representing the oscillation mode are  $\lambda_{1,2} = -0.015 \pm j3.5316$ . The magnitudes of elements of the right-eigenvectors that correspond to  $\Delta f_1$  and  $\Delta P_{T12}$  are 0.6088 and 0.1953, respectively. As a result,  $\Delta f_1$  provides higher degree of activity in this mode. Consequently,  $\Delta f_1$  is used as the input signal of SSSC controller. The negative feedback control scheme of SSSC controller can be expressed by

$$\Delta P_{ref} = -K_{RB}(s)\Delta f_1 \tag{19}$$

The robust controller  $K_{RB}(s)$  is in form of a lead/lag stabilizer as

$$K_{RB}(s) = k \frac{T_w s}{1 + T_w s} \frac{(1 + T_1 s)(1 + T_3 s)}{(1 + T_2 s)(1 + T_4 s)}$$
(20) 276

where k: a controller gain,  $T_1$ ,  $T_2$ ,  $T_3$ ,  $T_4$ : lead/lag time constants (s),  $T_w$ : a washout time constant (s).

Here,  $T_n$  is set to 10 (s). The control parameters k,  $T_1$ , 278  $T_2$ ,  $T_3$ ,  $T_4$  and  $T_4$  are searched based on the objective function explained in the next section. 280

### RTICLE IN PRESS

I. Ngamroo, W. Kongprawechnon I Electric Power Systems Research xxx (2003) xxx-xxx

Fig. 3. Feedback system with multiplicative uncertainty.

#### 3.3.2. Determination of objective function

In derivation of the objective function, both attenuation performance of system disturbances, and robust stability of controller against system uncertainties are taken into consideration. Since the main purpose of SSSC is to limit the peak frequency deviation following a sudden load perturbation, the peak frequency deviation can be used as a design specification. Assume that the eigenvalues corresponding to the mode of frequency oscillation in the uncontrolled system G are determined as  $-\sigma \pm j\omega_d$ . Thus, the system peak response to the unit step input is given by

$$M_{P(actual)} = 1 + \exp(-\sigma \pi/\omega_d)$$
 (21)

[15]. If the peak allowable frequency deviation of the controlled system is specified to be  $M_{P(design)}$ , then the magnitude of the difference between the design and the actual peak frequency deviations can be defined as

$$\dot{\psi} = |M_{P(design)} - M_{P(actual)}| \tag{22}$$

This is the part of disturbance attenuation performance in the objective function that will be minimized.

Next, the robust stability against system uncertainties is taken into consideration. The possible uncertainties are ignored nonlinear characteristics of the study system, ranges and bounds for uncertain system parameters etc. Practically, it is hardly to know about the information of all uncertainties existing in the system. To consider such system uncertainties, the unstructured uncertainty can be applied. In general, an upper bound of the magnitude (or size) of unstructured uncertainty can be estimated. If the magnitude of system uncertainties is less than this upper bound, the robust stability of system is guaranteed. Here, the multiplicative uncertainty [15] is applied to represent the unstructured uncertainty in the system, as shown in Fig. 3. Note that G is a nominal system transfer function,  $\Delta_m$  is a stable multiplicative perturbation, and K is a controller designed to ensure the internal stability of the nominal closed loop. Based on the small-gain theorem [15], the closed loop system will be robustly stable if

$$|\Delta_m| < \frac{1}{|GK(1+GK)^{-1}|}$$
 (23)

where, the symbol  $|\Delta_{\rm m}|$  shows the magnitude of uncertainty.  $|GK(1+GK)^{-1}|$  is the magnitude of complementary sensitivity function which is referred to as |T|.

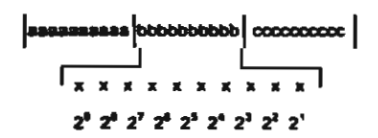


Fig. 4. Example of a 30 bit concatenated encoding scheme

margin (MSM) is defined as 322  $MSM = 1/||T||_{\infty}$ (24) 323

As mentioned in [15], the multiplicative stability

where  $||T||_{\infty}$  is the  $\infty$ -norm of T. The MSM can be used to measure the robust stability of the system. Large value of MSM exhibits high robust stability of the system.

From (23) and (24), it is cleared that if the controller K can be designed to minimize  $||T||_{\infty}$ , the MSM increases. As a result, the upper bound of  $|\Delta_m|$  is enlarged, and the high robust stability will be ensured. Thus, the robustness index in the objective function can be defined in normalized form as,

$$\gamma = ||T||_{\infty}/||T||_{\infty(\text{initial})} \tag{25}$$

where  $||T||_{\infty \text{(initial)}}$  is the  $\infty$ -norm of T at the initial solution of search process.

Combining (22) and (25), the objective function F can be formulated as,

Minimize 
$$F = c \cdot \psi + \gamma$$
  
subject to  $k_{\text{mun}} \le k \le k_{\text{max}}$   
 $T_{i,\text{min}} \le T_i \le T_{i,\text{max}}$  (26) 337

The constant coefficient "c" is used to weight  $\psi$ -term, so that  $c \cdot \psi$  dominates  $\gamma$  during the parameters optimization. Note that, since  $\gamma$  is normalized to 1 at the initial solution, it is easy to find the value of "c" so that  $c \cdot \psi$  is greater than 1. Eventually, the search process minimizes both terms until  $c \cdot \psi$  meets the design specification and  $\gamma$  decreases to the possible minimum value. The minimum and maximum values of the gain k are set as 0.1 and 500, respectively. The minimum and maximum values of the time constants  $T_I$  (i=1, 2, 3, 4) are set as 0.01 and 5, respectively. In this research, TSA is employed to solve this optimization problem and search for optimal parameters of controller.

#### 3.3.3. TSA for parameter determination [6]

The TSA is a promising tool for solving combinatorial optimization problem. The algorithm is an iterative improvement procedure that can start from any initial solution. Three basic components of TSA are used as follows: the trial solution generation, tabu list (TL) restriction, and termination criterion.

The concatenated encoding method is employed as shown in Fig. 4.

399

400

401

402

403

404

405

406

**4**07

408

409

410

411

412

413

414

426

427

478

429

430

431

432

433

434

435

436

437

438

439

440

441

447

443

444

445

446

447

1. Ngamroo, W. Kongprawechnon | Electric Power Systems Research xxx (2003) xxx-xxx

Initial Solution: 100101101011000110101110010011 Trial Solution 1: 000101101011000110101110010011 Trial Solution 2: 1401011010110001101011110010011 Trial Solution 3: 10 101010101010101101110010011

Fig. 5. Example of generating trial solutions.

Fig. 6. Mechanism of TL.

359

360

361

362

363

364

365

366

367

368

369

370

371

372

373

374

375

376

377

378

380

381

382

383

384

385

386

387

388

389

390

391

392

393

394

395

396

397

Each parameter is encoded in a binary string normalized over its range. This encoding method stacks each normalized string in series with each other to construct the string individual. The same number of n bits is used to represent each parameter string.

To obtain the actual value of each parameter (27) is used to decode each normalized string to its decimal value for objective function evaluation.

$$P_{i} = P_{i,\min} + \frac{B_{i} \times [P_{i,\max} - P_{i,\min}]}{2^{n} - 1}$$
 (27)

where  $P_i$  is the actual value of the i-th parameter,  $P_{i, min}$ is the minimum value of the *i*-th parameter.  $P_{i,max}$  is the maximum value of the i-th parameter,  $B_i$  is the decimal integer value of binary string of the i-th parameter, and n is the number of bits representing each parameter. In the design process, 10 bits are used to represent each parameter.

To generate a trial solution of an initial feasible solution, one bit of binary string is flipped at a time. The maximum number of trial solutions per iteration is referred to a neighborhood solution space (NS). In this study, NS is set to 95% of the total number of bits [  $0.95 \times n \times N$  where N is a number of parameter searched.

The example of generating trial solutions is shown in Fig. 5.

The TL is referred to as an adaptive memory. The mechanism of TL is to keep attributes (bit positions) that created the best solution of the past iterations in the TL for a certain period. The attributes included in the TL cannot be used to create new solution candidates as long as they are in the TL. As the iteration proceeds, a new attribute enters into the TL as a fixed attribute. At the same time, the oldest attribute is released from the TL and becomes a free attribute, as illustrated in Fig. 6.

In particular, a size of TL affects the quality of the solution. It controls the search process to avoid being trapped in local optima. Note that the size of TL or socalled the tabu length, is only the control parameter of TSA. Basically, the tabu length that provided good solutions usually grows with the size of the problem.

However, observing the quality of the solution can identify the appropriate tabu length. If the tabu length is too small, the cycling of solution occurs in the search process. On the other hand, if the size is too large, the search process is too restricted and may deteriorate the solution. Here, the tabu length is set to  $[0.7 \times n \times N]$ .

Termination criterion refers to the condition that the search process will terminate. In the design, the search will terminate when the number of iterations reaches

To apply the TSA for optimal parameter determination, the initial feasible solution is generated arbitrarily. A move to a neighbor solution is performed if the TL does not restrict it. The best solution is updated during the search process until the termination criterion is satisfied. The following notations is used for the TSA procedure:

TL:	the tabu list,	416
NS:	the neighborhood solution space,	417
F(X):	the objective function of solution $X$ ,	418
$F_b^k$ :	the best objective function at iteration $k$ ,	419
$F_b^k$ : $X_o^k$ :	the initial feasible solution at iteration $k$ ,	420
$X_m^k$ :	a trial m solution at iteration k,	421
$X_{ch}^{k}$ :	the current best trial solution at iteration $k$ .	423
$X_{cb}^k$ : $X_b^k$ :	the best solution reached at iteration k,	423
kmax:	the maximum allowable number of iterations.	424
	bu search procedure can be described as follows:	425

- Read the constraints of searched parameters, the initial feasible solution  $X_a^k$ , and specification of the controller.
- Specify the length of TL,  $k_{max}$ , and size of NS.
- Initialize iteration counter k and empty TL. 3)
- Set  $X_b^k = X_a^k$ .
- Execute tabu search procedure:
  - 5.1 Initialize the trial counter m to zero.
  - Generate a trial solution  $X_m^k$  from  $X_n^k$ . 5.2
  - 5.3
  - If  $X_m^k$  is not feasible, go to 5.8. If  $X_m^k$  is the first feasible solution, set  $X_{cb}^k =$  $X_m^k$ .
  - Perform the tabu test. If  $X_n^k$  is tabued, then go 5.5 to 5.8.
  - 5.6 If  $F(X_m^k) < F(X_{cb}^k)$ , set  $X_{cb}^k = X_m^k$ . 5.7 If  $F(X_m^k) < F(X_b^k)$ , set  $X_c^k = X_m^k$ .

  - If m is less than NS, m = m+1 and go to 5.2.
  - If there is no feasible solution, set  $X_o^{k+1} = X_b^k$ . Otherwise, set  $X_o^{k+1} = X_{ch}^k$ , and update TL.
- 6) If  $k < k_{max}$ , then k = k + 1, and go to 5.
- 7)  $X_b^*$  is the best solution found.

#### 4. Simulation results and evaluation

To determine five control parameters by the TSA, the 448 values of N. NS and the tabu length are set to 5, 47 and 449

### TICLE IN PRESS

I. Ngamroo, W. Kongprawechnon I Electric Power Systems Research xxx (2003) xxx-xxx

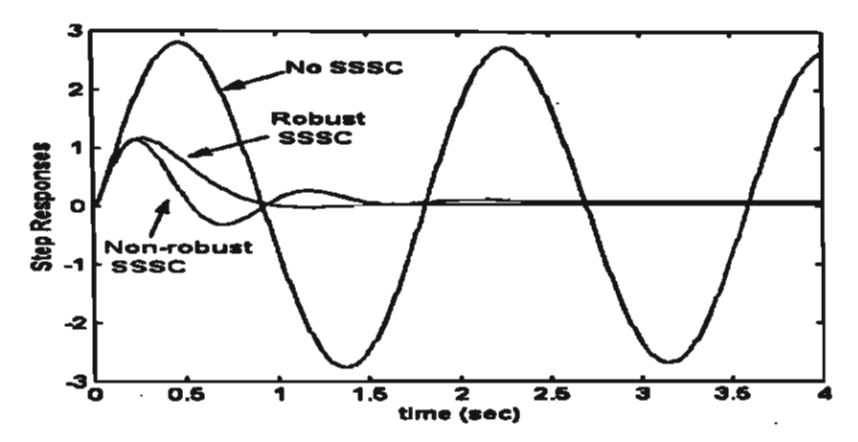


Fig. 7. System step responses

Table 1
Eigenvalue analysis results of decoupled subsystems (15) and (16)

	Before control	After control
Decoupled subsystem (15)	$\lambda_{1,2} = -0.015 \pm j 3.5316$	$\lambda_{1,2} = -3.6077 \pm j3.7967$
, , , , , , , , , , , , , , , , , , , ,		$\lambda_{3.4} = -0.1027 \pm j0.0642$
		$\lambda_5 = -0.5020$
		$\lambda_6 = -12.8613$
Decoupled subsystem (16)	$\lambda_{1,2} = -0.0152 \pm j  1.6777$	Not change
•	$\lambda_{3.4} = -0.0168 \pm j 3.6922$	
	$\lambda_{5.6} = -0.0247 \pm j 2.1532$	

35, respectively. Following the design procedures and appropriately setting c = 1.4 in the objective function, the following transfer function was obtained for the robust controller of SSSC when the peak frequency deviation was limited to  $M_{P(design)} = 1.2$ .

455 
$$K_{RB}(s) = 3.5206 \frac{10s}{1 + 10s} \frac{(1 + 0.7758s)(1 + 1.9660s)}{1 + 2.5074s(1 + 3.7269s)}$$
 (28)

The SSSC controller in Eq. (28) is compared with the designed SSSC with  $M_{p,(design)} = 1.2$  but without robustness consideration. By neglecting  $\gamma$  in the objective function and setting c = 1.0, the designed result is given by

460 
$$K_{NRB}(s) = 5.4753 \frac{10s}{1 + 10s} \frac{(1 + 0.1271s)(1 + 3.8781s)}{(1 + 2.7026s)(1 + 2.4440s)}$$

(29)

Note that the designed controllers in Eqs. (28) and (29) are referred to as "Robust SSSC" and "Non-robust SSSC", respectively.

Table 2
Eigenvalue analysis results of expanded system (12) (or interconnected overlapping subsystems (13) and (14))

	Before control	After Control
Expanded system (12)	$\lambda_{1,2} = -0.0171 \pm j4.4134$	$\lambda_{1,2} = -3.8240 \pm j5.0223$
	$\lambda_{3,4} = -0.0184 \pm j3.5602$ $\lambda_{5,6} = -0.0157 \pm j1.7520$ $\lambda_7 = -0.0409$ $\lambda_8 = -4.18 \times 10^{-14}$	$\lambda_{3,4} = -0.0461 \pm j3.6994$ $\lambda_{5,6} = -0.0061 \pm j1.7364$ $\lambda_7 = -0.0414$ $\lambda_8 = -2.84 \times 10^{-14}$ $\lambda_{9,10} = -0.1232 \pm j0.0483$ $\lambda_{11} = -0.4485$ $\lambda_{12} = -12.4$

Fig. 7 depicts the step responses of G. Without SSSC, the oscillations are undamped with the first peak value about 2.7875. On the other hand, the first peak values are reduced to 1.2025 and 1.1225 in cases of Robust and Ncn-robust SSSCs, respectively. In addition, the MSM of system G with Robust SSSC is increased to 0.90 from 0.57 in case of system with Non-robust SSSC. This reveals the higher robustness of the system G with Robust SSSC.

To prove that the Robust SSSC designed in the decoupled subsystem (15) can guarantee the stability of the expanded system (12) and also the original system (10), the eigenvalue analysis is employed. Table I shows the eigenvalues of decoupled subsystems (15) and (10). The eigenvalues  $\lambda_{1,2}$  of (15) represent the inter-area mode between areas I and 2. After applying the control input  $\Delta P_{\rm SSSC}$ , this oscillation mode is stabilized effectively. On the other hand, eigenvalues of (16) have not been changed. This is due to no control input  $\Delta P_{\rm SSSC}$  in (16). Table 2 shows the eigenvalues of expanded system (12). By considering the participation factor [14], it can be verified that  $\lambda_{1,2}$  represents the inter-area mode between areas I and 2. As expected,  $\Delta P_{\rm SSSC}$  can stabilize this oscillation mode. For other modes, they are stable

500

501

502

503

504

505

506

507

508

509

510

511

512

513

514

515

517

518

519

520

521

522

523

524

525

526

527

528

529

530

531

532

533

534

536

537

538

### ARTICLE IN PRESS

1. Ngamroo, W. Kongprawechnon I Electric Power Systems Research xxx (2003) xxx-xxx

Table 3
Eigenvalue analysis results of original system (11)

	Before control	After control
Originai system (11)	$\lambda_{1,2} = -0.0171 \pm j4.4134$	$\lambda_{1.2} = -3.8240 \pm j5.0223$
	$\lambda_{3,4} = -0.0184 \pm j3.5602$	$\lambda_{3,4} = -0.0461 \pm j 3.6994$
	$\lambda_{5,6} = -0.0157 \pm j 1.7520$	$\lambda_{5,6} = -0.0061 \pm j 1.7364$
	$\lambda_7 = -0.0409$	$\lambda_7 = -0.0414$
		$\lambda_{8.9} = -0.1232 \pm j0.0483$
		$\lambda_{10} = -0.4485$
		$\lambda_{11} = -12.4217$

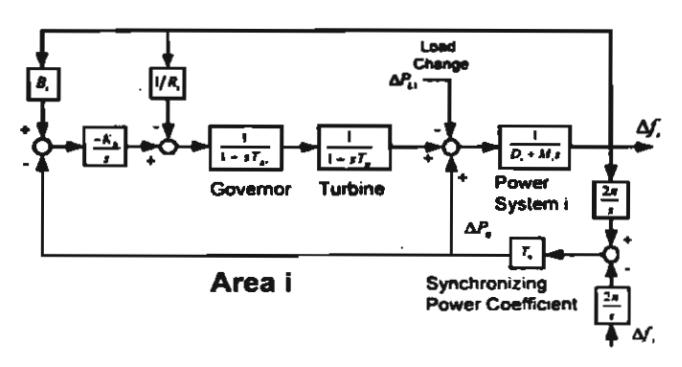


Fig. 8. Linearized model of area i (i = 1, ..., 4) with governor

487

488

489

490

491

492

493

494

495

496

497

498

after the controller is included. Note that  $\lambda_B$  is approximately zero which has no physical meaning. This is because of a redundant state variable  $\Delta P_{T12}$  in (12). For the eigenvalues of the original system (11) demonstrated in Table 3,  $\lambda_{1,2}$  can also be stabilized by  $\Delta P_{SSSC}$ . Other modes are also stable after control. These eigenvalue analysis results confirm the concept of overlapping decompositions that the stability of the original system can be guaranteed if the decoupled subsystems can be stabilized by its own input.

Next, the disturbance attenuation performance and robustness of both designed controllers are investigated

in the linearized model of the four-area interconnected system. The dynamic of governor [12] is also incorporated into each area, as delineated in Fig. 8. System parameters are given in the Appendix A.

In order to evaluate the disturbance attenuation performance of both controllers, a sudden step load of 0.01 (p.u. MW) is applied to area 1 at t = 1.0 (s). The frequency deviation of each area is depicted in Figs. 9-12. Without control of the SSSC, the fluctuations of frequency deviations in all areas are large with poor damping. After the inclusion of both controllers, frequency oscillations in all areas are effectively stabilized. Especially, the peak value of frequency deviation in the controlled area 1 is significantly suppressed. In addition, the oscillating shapes are also stabilized completely. Meanwhile, steady-state errors of frequency deviations are eliminated slowly due to the effects of the governors. Furthermore, the tie line 1-2 power deviation illustrated in Fig. 13 is also effectively stabilized by Robust SSSC. As shown in Fig. 14, the maximum injected power deviation of Non-robust SSSC is 0.0094 (p.u. MW), which is almost equal to the size of load change. In contrast, due to consideration of both performance and robustness in design process, the injected power deviation of Robust SSSC is 0.0058 (p.u. MW).

Here, the robustness of each designed controller is evaluated. A random load disturbance composed of several oscillation frequencies,  $\Delta P_{L1} = 0.002 \sin(3t) + 0.005 \sin(6t) - 0.007 \sin(9t)$  (p.u. MW) is applied to area 1. At the same time, the damping coefficient in area 1 ( $D_1$ ) is changed from 0.006 (p.u. MW/Hz) (positive damping) to -0.75 (p.u. MW/Hz) (negative damping). Note that the negative damping signifies an unstable system operation. As clearly illustrated by the area 1 frequency oscillations in Fig. 15, the system completely loses stability in cases of a Non-robust SSSC and no SSSC. Moreover, frequency oscillations in other areas (not shown here) severely fluctuate and finally diverge. On the other hand, the Robust SSSC explicitly

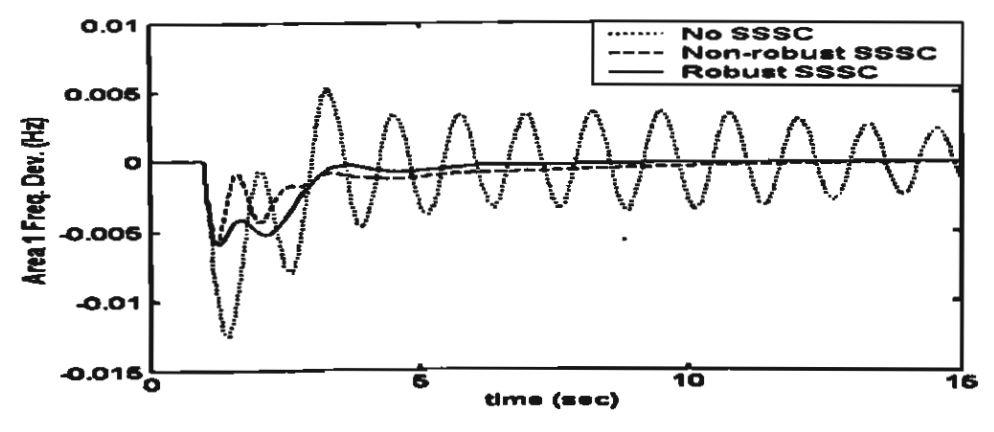


Fig. 9. Frequency deviation of area 1.

### APTICLE IN PRESS

1. Ngumroo, W. Kongprawechnon / Electric Power Systems Research xxx (2003) xxx-xxx

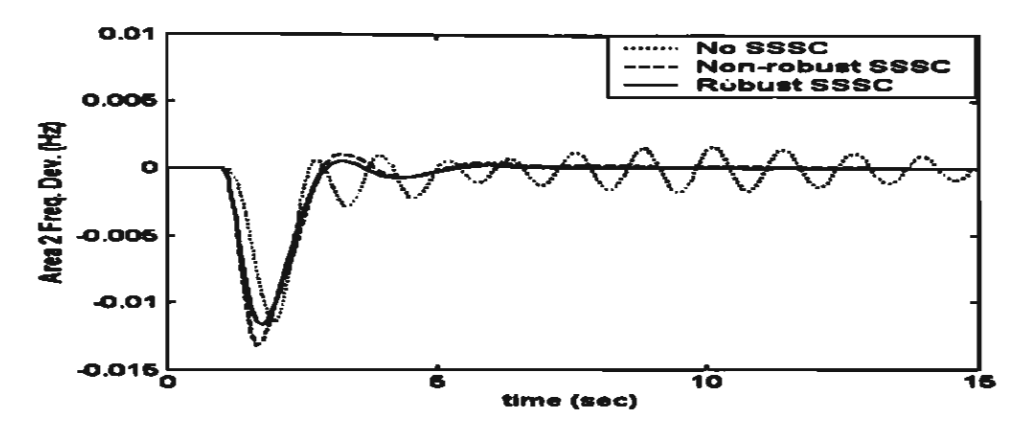


Fig. 10. Frequency deviation of area 2.

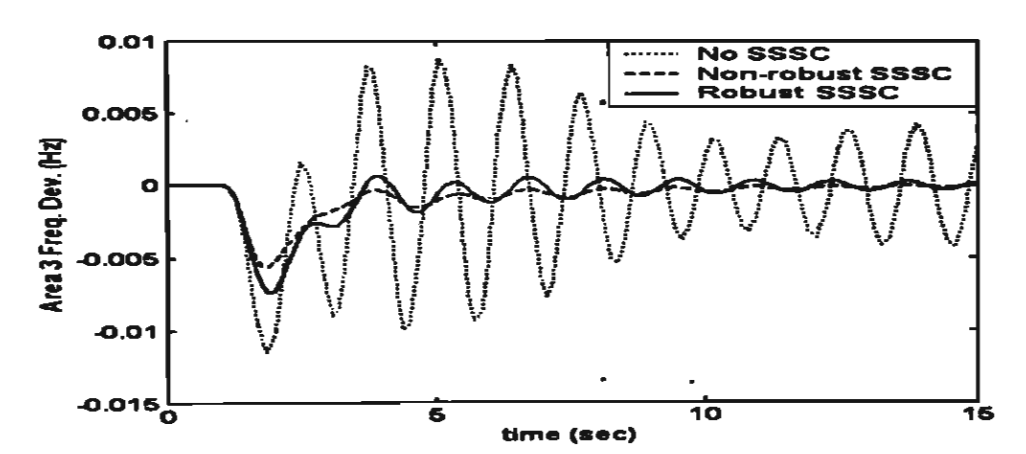


Fig. 11. Frequency deviation of area 3.

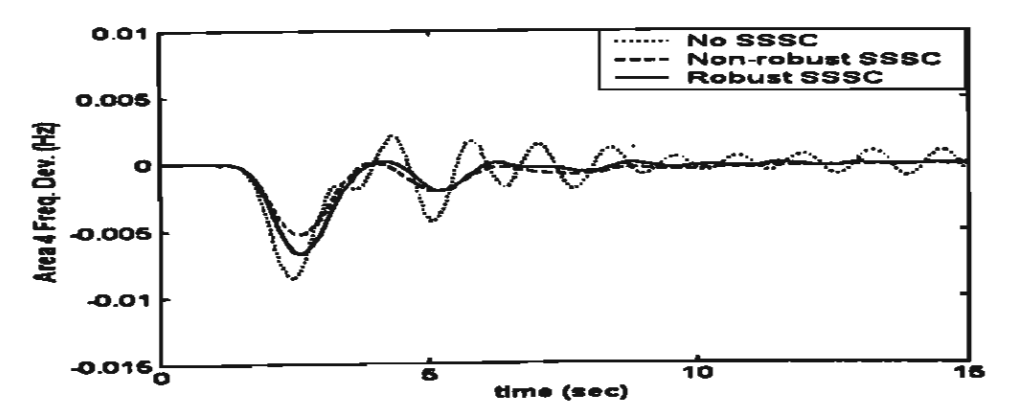


Fig. 12. Frequency deviation of area 4.

maintains its performance against large uncertainties and severe perturbations. Frequency oscillations in area I and other areas are perfectly stabilized. The efficiency of the Robust SSSC is also evident in Figs. 16 and 17, where the power deviation in the tie line 1-2 and the injected power deviation of SSSC are shown.

Finally, the performances of both SSSC controllers are evaluated when the load change occurs in area 2. Fig. 18 shows an additional load change in area 2. It is assumed that a sudden step load of 0.01 (p.u. MW) occurs in area 2 at t = 1.0 (s). As depicted in Fig. 19, both Non-robust SSSC and Robust SSSC are capable of

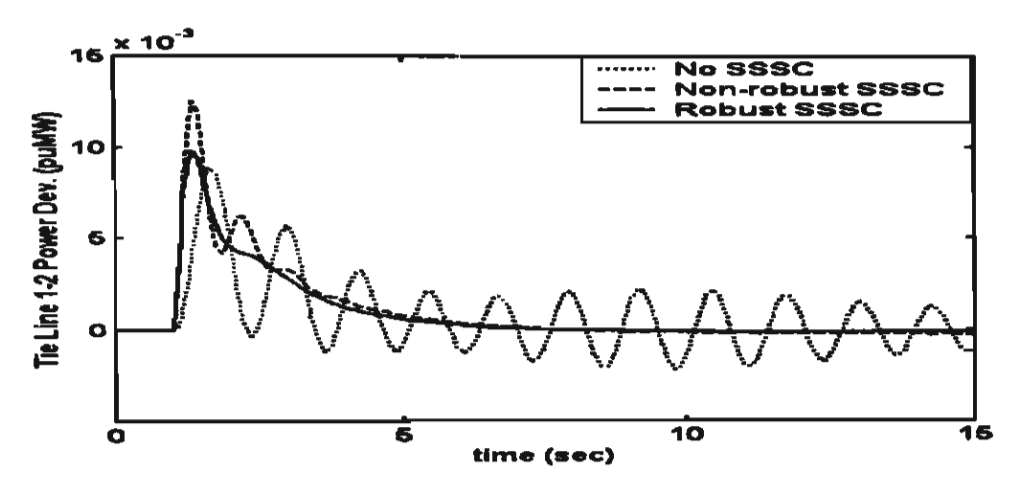


Fig. 13. Tie line 1-2 power deviation.

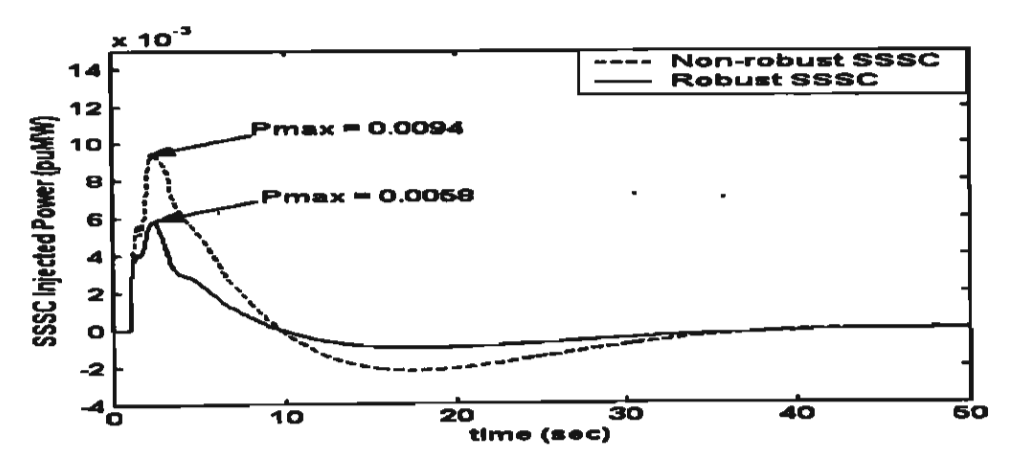


Fig. 14. Injected power deviation of SSSC.

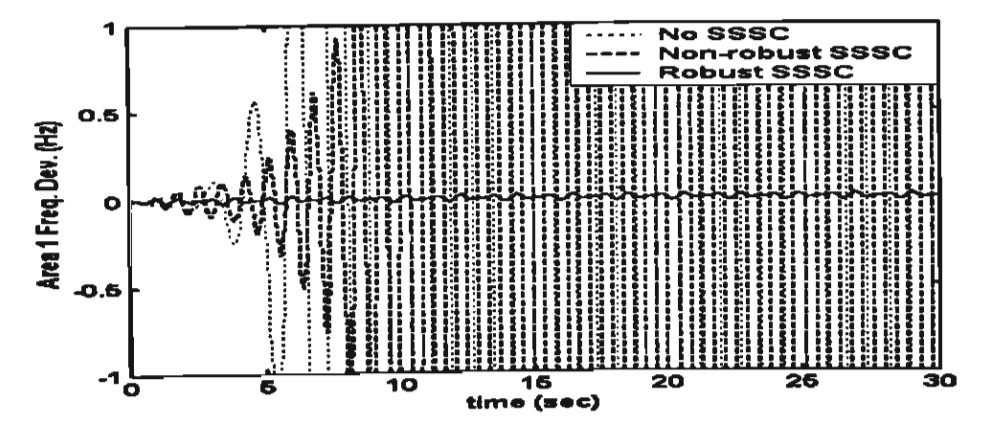


Fig. 15. Frequency deviation of area 1.

### TICLE IN PRESS

1. Ngamroo, W. Kongprawechnon ! Electric Power Systems Research xxx (2003) xxx-xxx

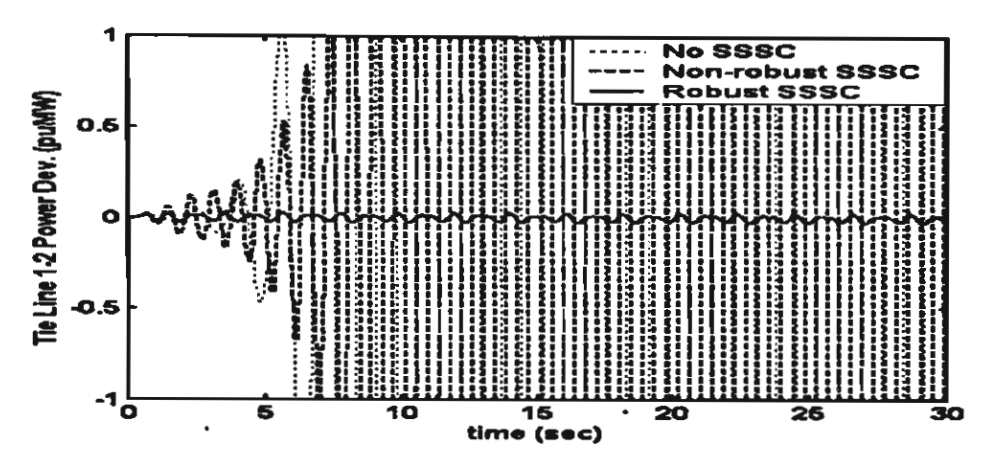


Fig. 16. Tie line 1-2 power deviation.

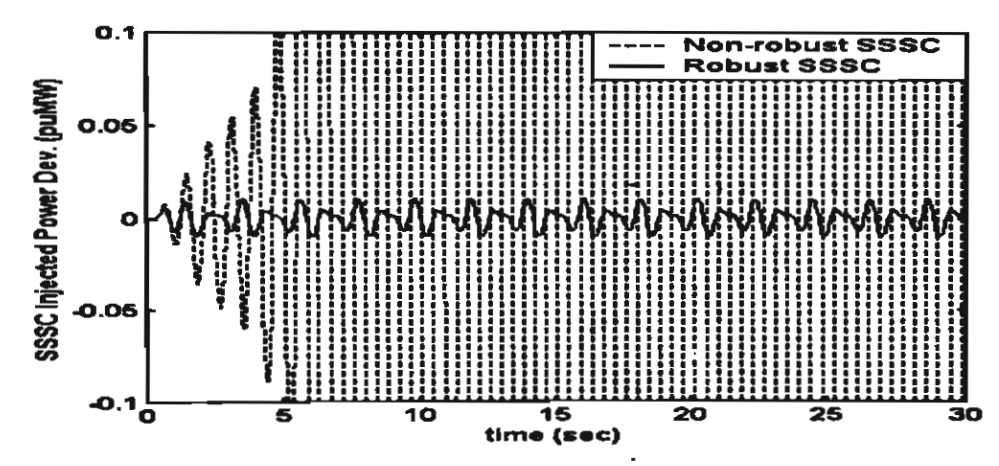


Fig. 17. Injected power deviation of SSSC.

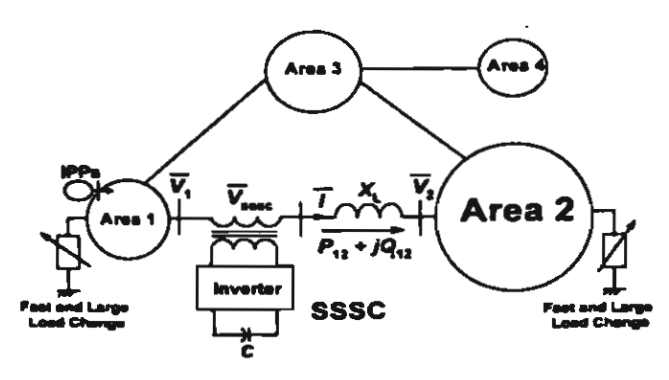


Fig. 18. An additional load change in area 2.

stabilizing frequency oscillations of area 1, even though a load disturbance occurs in area 2. For frequency deviations in other areas (Figs. 20-22) and tie line 1-2 power deviation (Fig. 23), the performance of Robust SSSC is comparatively better than that of Non-robust SSSC. As illustrated in Fig. 24, the peak values of

injected power deviations of Robust SSSC and Non-robust SSSC are 0.01 and 0.027 (p.u. MW), respectively. This implies that the required MW capacity of Robust SSSC is lower than that of Non-robust SSSC.

#### 5. Conclusions

In this paper, a robust design of the lead/lag controller equipped with the SSSC for stabilization of frequency oscillations is proposed. The TSA was employed to achieve the optimal parameters. By virtue of the objective function that limits the peak frequency deviation and maximizes the robust stability margin, the proposed design guarantees both performance and robustness of the resulted controller. More specifically, the designed controller uses only the frequency deviation of the controlled area as the feedback—input signal. This allows practical realization and implementation in a power system. Simulation results clearly demonstrate

### RTICLE IN PRESS

I. Ngamroo, W. Kongprawechnon I Electric Power Systems Research xxx (2003) xxx-xxx

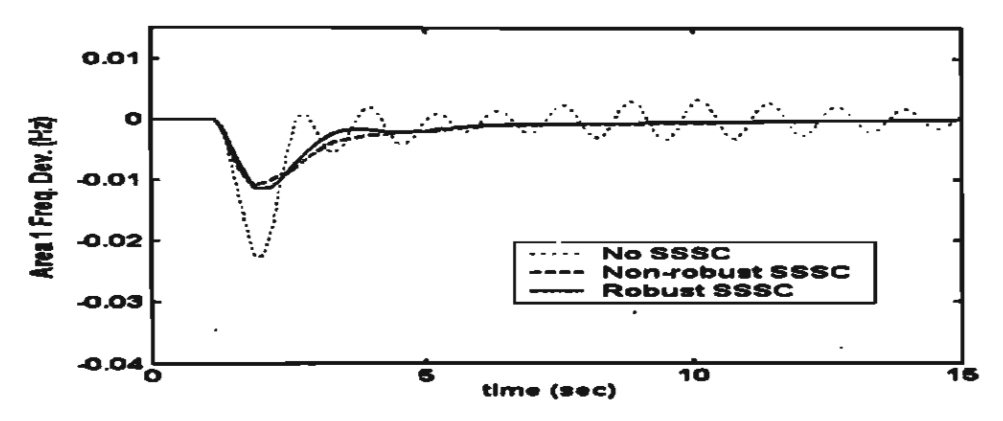


Fig. 19. Frequency deviation of area 1.

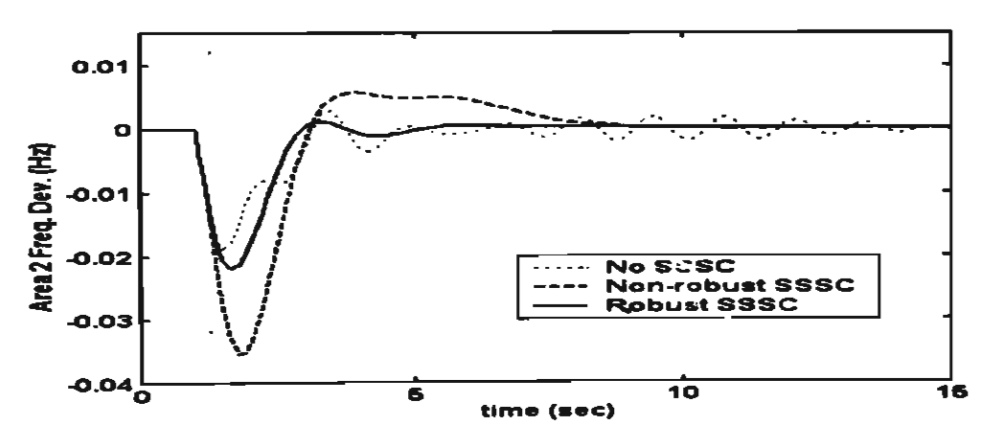


Fig. 20. Frequency deviation of area 2.

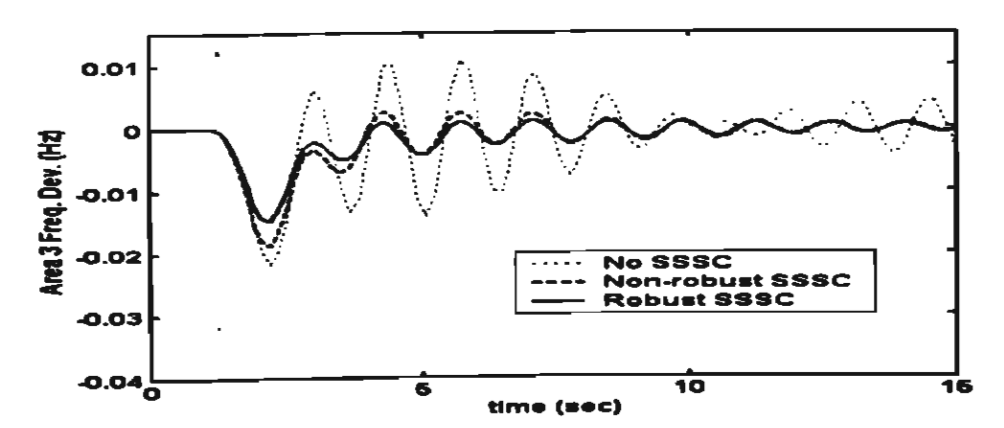


Fig. 21. Frequency deviation of area 3.

1. Ngamroo, W. Kongprawechnon I Electric Power Systems Research xxx (2003) xxx-xxx

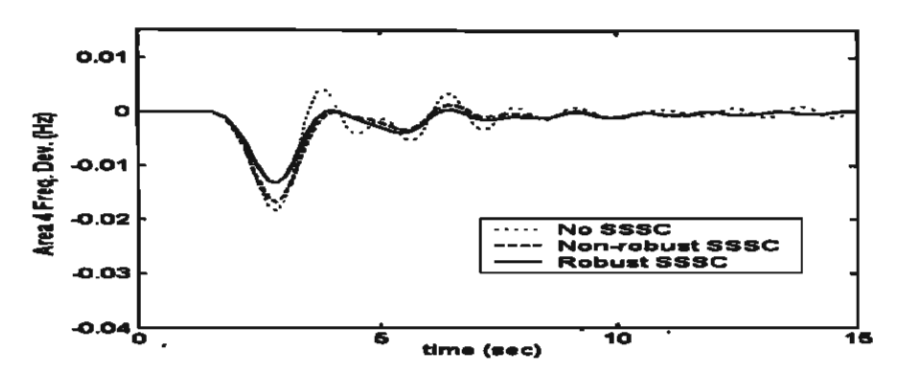


Fig. 22. Frequency deviation of area 4.

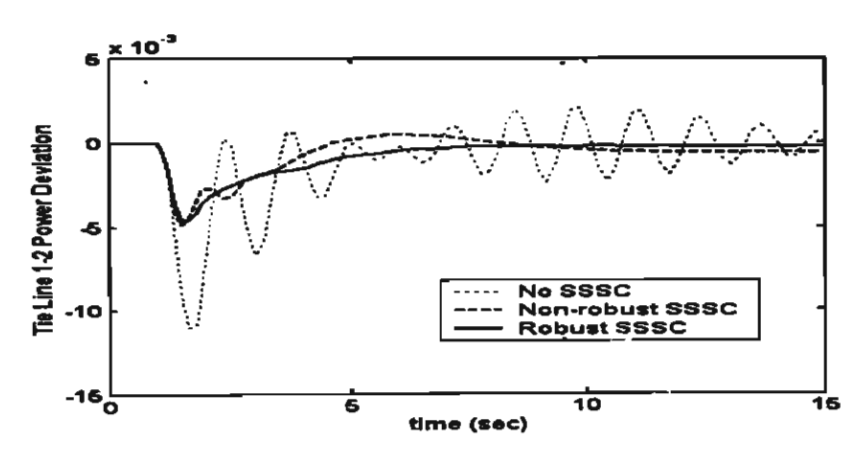


Fig. 23. Tie line 1-2 power deviation.

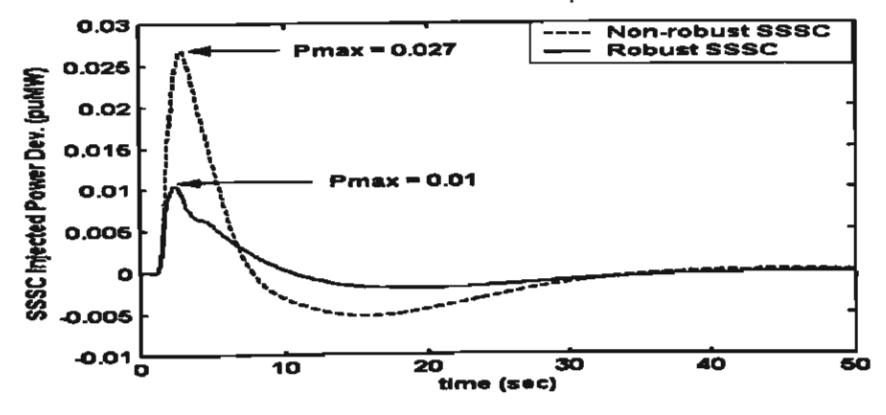


Fig. 24. Injected power deviation of SSSC.

the superior robustness and performance of the con-90 troller designed by the proposed method.

#### Acknowledgements

192

593

594

595

504

997

611

612

623

628

629

630

The authors deeply appreciate the support from this Thelland Research Fund through the postdoctoral fund program

### Appendix A

The system parameters of the four-area interconnected system with an area capacity ratio 5:10.2:0.8 are given below

601	$M_1 = 0.2$	$M_2 = 0.167$	M = 0.15	$M_4 = 0.2$
602	$D_1 = 0.006$	$D_2 = 0.0083$	$D_3 = 0.005$	$D_4 = 0.006$
603	$T_{c3} = 0.25$	$T_{12} = 0.3$	$T_{i,j} = 0.3$	$T_{r4} = 0.25$
604	$T_{e1} = 0.1$	$T_{e2} = 0.08$	$T_{e^{\lambda}} = 0.1$	$T_{e4} = 0.1$
605	$R_1 = 2.4$	$R_2 = 2.4$	$R_1 = 2.4$	$R_4 = 2.4$
606	$B_1 = 0.5$	$B_{*} = 0.5$	$B_3 = 0.5$	$B_{\bullet} = 0.5$
607	$K_{11} = 0.5$	$K_{12} = 0.5$	$K_{13} = 0.5$	$K_{-4} = 0.5$
608	$T_{12} = 0.159$	$T_{21} = 0.064$	$T_{34} = 0.111$	$T_{31} = 0.079$
609	$a_{12} = 2.0$	$a_{23} = 0.2$	$a_{34} = 2.5$	$a_{\rm M}=0.4$
610	$T_{\rm SSSC} = 0.05$			

#### Appendix B: Nomenclature

614	$M_{I}$	mertia constant (p.u. MW s/Hz) of area i		
615	D,	damping coefficient (p.u. MW/Hz) of area i		
616	$T_{i}$	turbine time constant (s) of area i		
	-	and the second s		

governor time constant (s) of area i 617 7,

regulation ratio (Hz/p u MW) R. 618 bias coefficient (p.u. MW/Hz) B, 619

integral gain (i/s) 620

synchronizing coefficient (p.u. MW/rad) be-621 tween areas r and j

area capacity ratio between areas i and j 622

 $T_{SSSC}$ : time constant of SSSC (s)

#### References 624

- [1] K.N. Zadeh, R.C. Meyer, G. Cauley, Practices and new concepts 625 in power system control, IEEE Trans. Power Syst. 11 (1) (1996) 626 627 3-9
  - [2] L.H. Fink, P.J.M. Van Son, On system control within a restructured industry, IEEE Trans. Power Syst. 13 (2) (1998) 611-616
- [3] N. Jaleeli, L.S. VanSlyck, D.N. Ewart, L.H. Fink, A.G. Hoff-631 mann. Understanding automata, generation control, IEEE Trans. 632 633 Power Syst. 7 (3) (1992) 1106 - 1122.

- [4] I. Ngamroo, Application of static synchronous series compensation to stabilization of frequency oscillations in an interconnected power system, Proceedings of 2001 IEEE International Symposium on Circuits and Systems (ISCAS 2001), Sydney, Australia, 2001, vol. 2, pp. 113-116
- [5] L. Gyugyi, C.D. Schauder, K.K. Sen, Static synchronous series compensator a solidstate approach to the series compensation of transmission line, IEEE Trans. Power Deliv. 12 (1) (1997) 406-
- [6] F. Glover, M. Laguna, Tabu Search, Kluwer Academic Publishers, 2001
- [7] W. Ongsakul, P. Bhasaputra. Optimal power flow with FACTS devices by hybrid TS/SA approach, Intl. J. Elec. Power Energy Syst. 24 (10) (2002) B51 - B57
- [8] M.A. Abido, Y.L. Abdel-Magid, A tabu search based approach to nower system stability enhancement via excitation and static phase shifter control, Elec. Power Syst. Res. 52 (2) (1999) 133-141
- [9] H. Mori, T. Hiyashima, New parallel tabu search for voltage and reactive power control in power systems. Proceedings of 1998 IEEE International Symposium on Circuits and Systems (ISCAS 98) vol. 3, pp. 431 - 434
- [10] W.G. Kim, G.H. Hwang, H.T. Kang, S.O. Lee, J.H. Park, Design of fazzy logic controller for firing control of TCSC using real-type tabu search, Proceedings IEEE International Symposium on Industrial Electronics 2001 (ISIE 2001), vol. 1, pp. 575 -580
- [11] Y.L. Abdel Magid, M.A. Abido, A.H. Mantaway, Robust tuning of power system stabilizers in multimachine power systems, IEEE Trans. Power Syst. 15 (2) (2000) 735 - 740.
- [12] O.L. Elgerd, Electric Energy Systems Theory, An Intro-McGraw Hill, New York, USA 1985
- [13] M. Ikeda. D.D. Siljak, D.E. White. Decentralized control with overlapping information sets, J. Optimization Theor. Appl. 34 (2) (1981) 279 310
- [14] P.B. Kundur, Power System Stability and Control, McGraw-Hill, 1994
- [15] B. Shahian, M. Hassul, Control System Design using MATLAB, Prentice Hall 1993

#### Biographics

Issarachai Ngamroo received the B Eng. degree in Electrical Engineering from King Mongkut's Institute of Technology Ladkrabang (KMITL), Bangkok, Thailand in 1992. He was the recipient of a Monbusho scholarship from the Japanese Government to continue his graduate study in Japan during 1993 2000. He received his M.Eng and the Ph.D. degrees in Electrical Engineering in 1997 and 2000, respectively, from Osaka University, Osaka, Japan. He is currently an Assistant Professor at Electrical Power Engineering Program, Sirindhorn International Institute of Technology Thammasat University. His (SHT). research interests are in the areas of power system control stabilization. Flexible AC Transmission System Devices (FACTS) applications, Robust design οſ power damping control system controllers

Waree Kongprawechnon received the B.Eng. degree (1st Honors) in Electrical Engineering from Chulalongkorn University, Bangkok, Thailand. She received the

643

634

666 667 668

669 670 671

672 673

675

> 687 688 689

690 691 692 M /Elsevier Science/Shannon/EPSR/articles/EPSR1887/EPSR1887.3d[x]

20 June 2003 8:19:6

ARTICLE IN PRESS

I. Ngamroo, W. Kongprawechnon I. Electric Power Systems Research xxx (2003) xxx-xxx

M Eng in control engineering from Osaka University and the Ph D degrees in Mathematical Engineering and Information Physics from The University of Tokyo, Japan She is currently an Assistant Professor of the Instrumentation and Control Systems Program, Sirindhorn International Institute of Technology (SIIT), Thammasat University Her research interests are in the areas of the theory in robust control,  $H^{\infty}$  Control.

### Robust Frequency Stabilizer Design of Static Synchronous Series Compensator Taking into Consideration System Uncertainties

### Issarachai Ngamroo and Waree Kongprawechnon

Electrical Power Engineering Program
Sirindhorn International Institute of Technology
Thammasat University, Pathumthani, 12121 Thailand
E-mail: ngamroo@siit.tu.ac.th

#### **ABSTRACT**

As large loads with changing frequency in the vicinity of inter-area oscillation (0.2 - 0.8 Hz) mode occur in an interconnected power system, system frequency may be severely disturbed and oscillate To compensate for such load changes and stabilize both frequency oscillations, the dynamic power flow control via a Static Synchronous Series Compensator (SSSC) installed in series with a tie-line between interconnected systems can be exploited. However, the frequency stabilizer of SSSC that is designed without regarding system uncertainties, e.g., various load changes, system parameters variations etc., may deteriorate the robust stability of power system and fail to damp out low frequency oscillations. To overcome this problem, a new robust design of frequency stabilizer of SSSC taking into consideration system uncertainties is proposed. The multiplicative uncertainty model is applied to represent all possible unstructured uncertainties in interconnected power systems. As a result, the robust stability margin against uncertainties can be easily guaranteed in terms of the multiplicative stability margin (MSM). Additionally, to implement the frequency stabilizer in real system, the configuration of frequency stabilizer presented here is practically based on a second-order lead/lag compensator. Without trial and error, the control parameters of the frequency stabilizer are automatically optimized by a tabu search algorithm, so that the desired damping ratio of the target inter-area mode and the best MSM are achieved. Simulation study exhibits the high robustness of the SSSC frequency stabilizer against load disturbances with changing frequency in the vicinity of the inter-area and negative damping in the study three-area loop interconnected power system.

Keywords: System uncertainties, Robust stability, Multiplicative uncertainty model, Static synchronous series compensator, Inter-area oscillations, Frequency stabilization, Overlapping decompositions, Tabu search algorithm

#### 1. INTRODUCTION

At present, an electric power system is in transition to a fully competitive deregulated scenario. Under this circumstance, any power system controls such as frequency and voltage controls will be served as ancillary services [1-3]. Especially, in the case that the proliferation of non-utility generations, i.e. Independent Power Producers (IPPs) that do not possess sufficient frequency control capabilities, tends to increase considerably. Furthermore, various kinds of apparatus with large capacity and fast power consumption such as a magnetic levitation transportation, a testing plant for nuclear fusion, or even an ordinary scale factory like a steel manufacturer etc. increase significantly. When these loads are concentrated in a power system, they may cause a serious problem of frequency oscillation. The

deviations of frequency oscillations that exceed the normal limit, directly interrupt the operation of power system. Especially, if the frequency of changing load is in the vicinity of the inter-area oscillation mode (0.2-0.8 Hz), system frequency oscillation may experience a serious stability problem due to an inadequate damping. Under this situation, the conventional frequency control, i.e. a governor, may no longer be able to absorb the large frequency oscillations due to its slow response [4, 5]. A new service of stabilization of frequency oscillations becomes challenging and is highly expected in the future competitive environment.

To solve this problem, the author has proposed a new stabilization of frequency oscillations by the Static Synchronous Series Compensator (SSSC) [6]. The SSSC is a FACTS (Flexible AC Transmission Systems) device, that has been highly expected as an effective apparatus with an ability of dynamic power flow control [7, 8]. In [6], the SSSC is located in series with the tie-line between a two-area interconnected power system. By regarding the system interconnection as the channel of power flow control by SSSC, the system frequency oscillations under a sudden load disturbance can be stabilized effectively. However, the proposed frequency stabilizer of SSSC in [6] is designed based on a state feedback scheme of variables. Therefore, it is not easy to realize in a multi-area interconnected power system. Besides, there are several uncertainties such as various load changes, system parameter variations etc. in interconnected power systems. The frequency stabilizer of SSSC that is designed without considering such uncertainties may deteriorate the robust stability of power system and fail to damp out low frequency oscillations.

By taking system uncertainties into consideration, a new robust frequency stabilizer of SSSC is proposed in this paper. The multiplicative uncertainty model [9-11] is applied to represent all possible unstructured uncertainties in interconnected power systems. As a result, the robust stability margin of the closed-loop control system can be easily guaranteed in terms of the multiplicative stability margin (MSM). First, the design method utilizes the merit of overlapping decompositions technique [12] to extract the subsystem embedded with the inter-area mode of interest. Next, by including the multiplicative uncertainty model in the extracted subsystem, the robust stability margin of system with designed frequency stabilizer can be enhanced. Here, the configuration of the robust frequency stabilizer is practically based on a second-order lead/lag compensator with single feedback input signal. Without trial and error, the control parameters of the robust frequency stabilizer are automatically optimized via a Tabu Search (TS) algorithm [13, 14]. In the formulation of the objective function, not only the desired damping ratio of the target inter-area mode, but also the MSM of system are included. In addition, the proposed method is applied to a design problem in case of many frequency stabilizers of SSSCs are installed in an interconnected power system. Simulation study in a three-area loop system shows the significant robustness of the designed frequency stabilizers against load changes and negative damping.

The organization of this paper is as follows. First, the motivation of stabilization of frequency oscillation by SSSC is provided. Next part deals with the design methodology including the coordinated control of SSSC and governors, the mathematical model of SSSC, the system reduction by overlapping decompositions, the objective function formulation, and the tabu search algorithm. Subsequently, the evaluation effects of the designed frequency stabilizers in a three-area interconnected power system are outlined by simulation study. Lastly, a conclusion is given.

#### 2. PROBLEM STATEMENT

A three-area loop interconnected power system depicted in Fig.1 is used to explain the motivation of the proposed frequency stabilizer design. SSSC12 and SSSC23 are connected in series with tie-lines between areas 1 and 2, and areas 2 and 3, respectively. It is assumed that large loads with changing frequency in the vicinity of the inter-area oscillation mode (0.2-0.8 Hz) have been installed in areas 1 and 3. These load disturbances severely cause frequency oscillations in areas 1 and 3. In addition, Independent Power Producers (IPPs) that do not possess frequency control capabilities are also included in areas 1 and 3. Thus, it becomes beyond the abilities of governors in areas 1 and 3 to

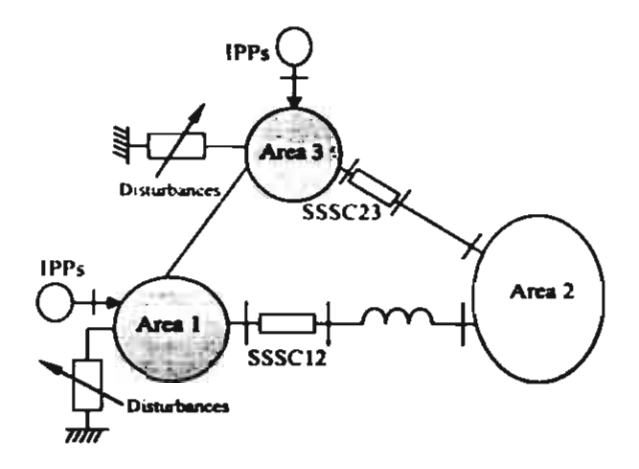


Figure 1: A three-area loop interconnected power system with SSSC

provide adequate frequency controls. Therefore, both SSSCs are applied to utilize the control capabilities of area 2 to compensate for fast load changes in areas 1 and 3. Moreover, by utilizing the area interconnections as the control channels of dynamic power flow control of SSSCs, the frequency oscillations in areas 1 and 3, due to inter-area modes can be effectively stabilized. Additionally, in the interconnected system, variations of system parameters, various load changes etc. cause several system uncertainties. To achieve the high robust stability of system, the effect of uncertainties should be taken into account in the design process. In this study, the aim of the proposed frequency stabilizer design is not only to enhance the damping of interested inter-area oscillation modes, but also to improve the robust stability of system against uncertainties.

# 3. Design Methodology

### 3.1 Coordinated Control of SSSC and Governor

The response of SSSC is extremely rapid when compared to the conventional frequency control system, i.e. a governor. The difference in responses signifies that the SSSC and governor can be coordinated. When a power system is subjected to a sudden load disturbance, the SSSC quickly acts to damp frequency oscillation in the transient period. Subsequently, the governor continues to eliminate the steady-state error in frequency oscillation. As the periods of operation for the SSSC and governor do not overlap, the dynamic of governor can then be neglected in the design of frequency stabilizer for the sake of simplicity.

## 3.2 Linearized Power System Model

The power system shown in Fig. 1 can be represented by a linearized power system model, as shown in Fig. 3. Note that the governors are eliminated in this system. The SSSC model is represented by the active power flow controller [6]. The dynamic characteristic of SSSC is modeled as the first order controller with a time constant  $T_{\text{SSSC}} = 0.05$  sec. Note that the injected power deviation of each SSSC ( $\Delta P_{\text{SSSC}(12)}$  and  $\Delta P_{\text{SSSC}(23)}$ ) acting positively on an area reacts negatively on another area [6]. Thus, each injected power flows into both areas with different signs (+,-), simultaneously. By neglecting  $T_{\text{SSSC}}$ , the linearized state equation of Fig. 3 can be expressed as

$$\Delta x = A\Delta x + B\Delta u \tag{1}$$

where

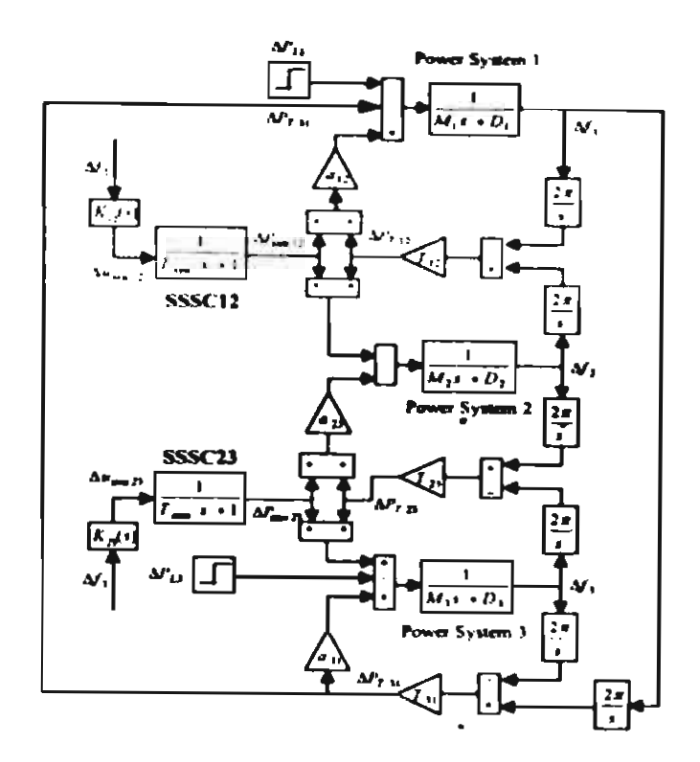


Figure 3. Frequency stabilizers of SSSCs in a linearized power system model without governors

$$A = \begin{bmatrix} -D_1/M_1 & a_{S12} & 0 & a_{S14} & 0 \\ -2\pi T_{12} & 0 & 2\pi T_{12} & 0 & 0 \\ 0 & -1/M_2 & -D_2/M_2 & -a_{23}/M_2 & 0 \\ 0 & 0 & 2\pi T_{23} & 0 & -2\pi T_{23} \\ 0 & a_{S32} & 0 & a_{S34} & -D_3/M_3 \end{bmatrix}.$$

$$B = \begin{bmatrix} a_{12}/M_1 & 0 \\ 0 & 0 \\ -1/M_2 & -a_{23}/M_2 \\ 0 & 1/M_3 \\ 0 & 0 \end{bmatrix}.$$

$$\Delta x = \begin{bmatrix} \Delta f_1 & \Delta P_{712} & \Delta f_2 & \Delta P_{723} & \Delta f_3 \end{bmatrix}^T,$$

$$\Delta u = \begin{bmatrix} \Delta P_{SSS(12)} & \Delta P_{SSS(23)} \end{bmatrix}^T.$$

 $\Delta f_{ij}$  is the frequency deviation of area i,  $\Delta P_{Tij}$  is the power deviation between areas i and j,  $M_i$  is the inertia constant of area i,  $D_i$  is the damping coefficient of area i,  $a_{ij}$  is the area capacity ratio between areas i and j,  $T_{ij}$  is the synchronizing power coefficient of the tie-line between areas i and j, where i, j = 1,...,3. Here  $a_{S/2} = (a_{12} + T_{1i}/T_{12})/M_i$ ,  $a_{S/4} = -T_{1i}/(M_1T_{2i})$ ,  $a_{SS2} = -a_{21}T_{1i}/(M_1T_{12})$ ,  $a_{SS4} = (1 + a_{21}T_{1i}/T_{2i})/M_j$ . The variable  $\Delta P_{TS1}$  is represented in terms of  $\Delta P_{TS2}$  and  $\Delta P_{TS3}$  by

$$\Delta P_{T11} = -\frac{T_{11}}{T_{11}} \Delta P_{T12} + \frac{T_{11}}{T_{21}} \Delta P_{T22}$$
 (2)

Thus,  $\Delta P_{731}$  has disappeared in (1). This system has two conjugate pairs of complex eigenvalues and a negative real eigenvalue. The former corresponds to two inter-area oscillation modes, and the latter the inertia center mode. Based on the mode controllability matrix [15], the inter-area modes between areas 1 and 2, and areas 2 and 3 are controllable for the control inputs  $\Delta u_{SSSC12}$  and  $\Delta u_{SSSC23}$ , respectively. Accordingly, the design purpose of frequency stabilizer is to enhance the damping of the mentioned inter-area modes.

#### 3.3 Model Reduction by Overlapping Decompositions

The technique of overlapping decompositions [12] is applied to reduce the system (1) to a subsystem embedded with only the inter-area mode of interest. The original system (1) is referred to as the system S.

$$S: \begin{bmatrix} \dot{x}_1 \\ \dot{x}_2 \\ \dot{x}_3 \end{bmatrix} = \begin{bmatrix} A_{11} & A_{12} & A_{13} \\ A_{21} & A_{22} & A_{23} \\ A_{31} & A_{32} & A_{33} \end{bmatrix} \begin{bmatrix} x_1 \\ x_2 \\ x_3 \end{bmatrix} + \begin{bmatrix} B_{11} & B_{12} \\ B_{21} & B_{22} \\ B_{31} & B_{32} \end{bmatrix} \begin{bmatrix} u_1 \\ u_2 \end{bmatrix}$$
(3)

The sub-matrices  $A_{ij}$  and  $B_{ij}$ , (i, j = 1, 2, 3) have appropriate dimensions identical to the corresponding states and input vectors. According to the process of overlapping decompositions, the system S can be expressed as

$$\tilde{S} : \begin{bmatrix} \dot{z}_1 \\ \dot{z}_2 \end{bmatrix} = \begin{bmatrix} A_{11} & A_{12} & 0 & A_{13} \\ A_{21} & A_{22} & 0 & A_{23} \\ A_{21} & 0 & A_{22} & A_{23} \\ A_{31} & 0 & A_{32} & A_{33} \end{bmatrix} \begin{bmatrix} z_1 \\ z_2 \end{bmatrix} + \begin{bmatrix} B_{11} \\ B_{21} \\ B_{31} \\ B_{31} \end{bmatrix} \begin{bmatrix} u_1 \\ u_2 \end{bmatrix} \tag{4}$$

where  $z_1 = \left[x_1^T, x_2^T\right]^T$  and  $z_2 = \left[x_2^T, x_3^T\right]^T$ . Subsequently, the system  $\tilde{S}$  can be decomposed into two interconnected overlapping subsystems, i.e.

$$\bar{S}_{1} : \dot{z}_{1} = \left( \begin{bmatrix} A_{11} & A_{12} \\ A_{21} & A_{22} \end{bmatrix} z_{1} + \begin{bmatrix} B_{11} \\ B_{21} \end{bmatrix} u_{1} \right) + \begin{bmatrix} 0 & A_{13} \\ 0 & A_{23} \end{bmatrix} z_{2} + \begin{bmatrix} B_{12} \\ B_{22} \end{bmatrix} u_{2}$$
 (5)

and

$$\bar{S}_{\frac{1}{2}} : \dot{z}_{2} = \left( \begin{bmatrix} A_{22} & A_{23} \\ A_{32} & A_{33} \end{bmatrix} z_{2} + \begin{bmatrix} B_{21} \\ B_{31} \end{bmatrix} u_{2} \right) + \begin{bmatrix} A_{21} & 0 \\ A_{31} & 0 \end{bmatrix} z_{1} + \begin{bmatrix} B_{21} \\ B_{31} \end{bmatrix} u_{1}$$
 (6)

The state variable  $x_2$  is repeatedly included in both subsystems, which implies "Overlapping Decompositions".

For system stabilization, two interconnected subsystems  $\tilde{S}_1$  and  $\tilde{S}_2$  are considered. The terms in the right hand sides of (5) and (6) can be separated into the decoupled subsystems (as indicated in the parenthesis in (5) and (6)) and the interconnected subsystems. As mentioned in [12], if each decoupled subsystem can be stabilized by its own input, the asymptotic stability of the interconnected overlapping subsystem  $\tilde{S}_1$  and  $\tilde{S}_2$  are maintained. Moreover, the asymptotic stability of the original system S is also guaranteed. Consequently, the interactions of the decoupled subsystems with the interconnection subsystems in (5) and (6) are regarded as perturbations. They can be neglected during control design. As a result, the decoupled subsystems of (5) and (6) can be expressed as

$$\tilde{S}_{D1}$$
:  $\dot{z}_{1} = \begin{bmatrix} A_{11} & A_{12} \\ A_{21} & A_{22} \end{bmatrix} z_{1} + \begin{bmatrix} B_{11} \\ B_{21} \end{bmatrix} u_{1}$  (7)

and

$$\tilde{S}_{112} : \dot{z}_{2} = \begin{bmatrix} A_{22} & A_{23} \\ A_{12} & A_{13} \end{bmatrix} z_{2} + \begin{bmatrix} B_{22} \\ B_{32} \end{bmatrix} u_{2}$$
(8)

By regarding the power deviation between areas 1 and 2 ( $\Delta P_{T12}$ ) as the overlapped variable for design of frequency stabilizer of SSSC12, the subsystem embedded with the inter-area mode between areas 1 and 2 can be expressed as

$$\vec{G}_{s1} : \begin{bmatrix} \Delta \dot{f}_1 \\ \Delta \dot{P}_{r12} \end{bmatrix} = \begin{bmatrix} -D_1/M_1 & a_{S12} \\ -2\pi T_{12} & 0 \end{bmatrix} \begin{bmatrix} \Delta f_1 \\ \Delta P_{r12} \end{bmatrix} + \begin{bmatrix} a_{12}/M_1 \\ 0 \end{bmatrix} \Delta P_{SSSC12}$$
(9)

Next, by considering the power deviation between areas 2 and 3 ( $\Delta P_{723}$ ) as the overlapped variable for design of frequency stabilizer of SSSC23, the subsystem embedded with the inter-area mode between areas 2 and 3 can be expressed as

$$\tilde{G}_{12}:\begin{bmatrix}\Delta\dot{P}_{123}\\\Delta\dot{f}_{1}\end{bmatrix}=\begin{bmatrix}0&-2\pi T_{23}\\a_{134}&-D_{3}/M_{3}\end{bmatrix}\begin{bmatrix}\Delta P_{123}\\\Delta f_{3}\end{bmatrix}+\begin{bmatrix}0\\1/M_{3}\end{bmatrix}\Delta P_{SSSC23}$$
(10)

By incorporating the dynamic characteristic of each SSSC as shown in Fig. 2, (9) and (10) become

$$G_{S1} : \begin{bmatrix} \Delta \dot{f}_{1} \\ \Delta \dot{P}_{T12} \\ \Delta \dot{P}_{SNSC12} \end{bmatrix} = \begin{bmatrix} -D_{1}/M_{1} a_{S12} & a_{12}/M_{1} \\ -2\pi T_{12} & 0 & 0 \\ 0 & 0 & -1/T_{SSSC12} \end{bmatrix} \begin{bmatrix} \Delta f_{1} \\ \Delta P_{T12} \\ \Delta P_{SSSC12} \end{bmatrix} + \begin{bmatrix} 0 \\ 0 \\ 1/T_{SSSC12} \end{bmatrix} \Delta u_{SSSC12}$$
 (11)

and

$$G_{S2} : \begin{bmatrix} \Delta \dot{P}_{723} \\ \Delta \dot{f}_{3} \\ \Delta \dot{P}_{SSSC23} \end{bmatrix} = \begin{bmatrix} -D_{1}/M_{1} a_{S12} & a_{12}/M_{1} \\ -2\pi T_{12} & 0 & 0 \\ 0 & 0 & -1/T_{SSSC23} \end{bmatrix} \begin{bmatrix} \Delta P_{723} \\ \Delta f_{3} \\ \Delta P_{SSSC23} \end{bmatrix} + \begin{bmatrix} 0 \\ 0 \\ 1/T_{SSSC23} \end{bmatrix} \Delta u_{SSSC23}$$
 (12)

where  $\Delta u_{SSSC12}$  and  $\Delta u_{SSSC23}$  are output signals of frequency stabilizers for SSSC12 and SSSC23, respectively. Equations (11) and (12) are used to design SSSC12 and SSSC23, respectively.

# 3.4 Structure of Frequency Stabilizer

In this study, the structure of the frequency stabilizer is based on a second-order lead/lag compensator as shown in Fig. 4.3. There are five parameters for each designed frequency stabilizer consisting of a stabilization gain K, time constants  $T_1, T_2, T_3$ , and  $T_4$ .

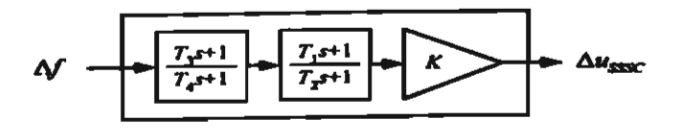


Figure 4. Configuration of 2nd order frequency stabilizer

Since the control purpose of the frequency stabilizer is to enhance the damping of the inter-area mode. The frequency deviation of each target area ( $\Delta f$ , i=1 and 3) which provides information of each mode of interest, is used as the input signal for each frequency stabilizer. The control parameters of each frequency stabilizer are optimized based on the following objective function.

## 3.5 Formulation of Objective Function

In deriving the objective function, not only the enhancement of system damping, but also the robust stability against system uncertainties are taken into consideration. Since the main purpose of the designed frequency stabilizer is to improve the system damping following any load disturbances, therefore, the damping ratio ( $\zeta$ ) of the inter-area mode is used as a design specification. Assuming that the eigenvalues corresponding to the mode of oscillation can be determined as  $-\sigma \pm j\omega_d$ , the damping ratio is given by

$$\zeta_{actual} = \frac{-\sigma}{\sqrt{\sigma^2 + \omega_d^2}} \tag{13}$$

The desired damping ratio of the eigenvalues corresponding to the mode of oscillation is specified as  $\zeta_{desired}$ . Accordingly, the difference between the desired and the actual damping ratios can be defined as

$$\alpha = \left| \zeta_{\text{desired}} - \zeta_{\text{actual}} \right| \tag{14}$$

For robust stability, the system uncertainties are modeled as a multiplicative form [9-11] demonstrated in Fig. 5.  $\tilde{G}$  is a system and  $\tilde{K}$  is a designed controller.  $\Delta_m$  is a stable multiplicative uncertainty.

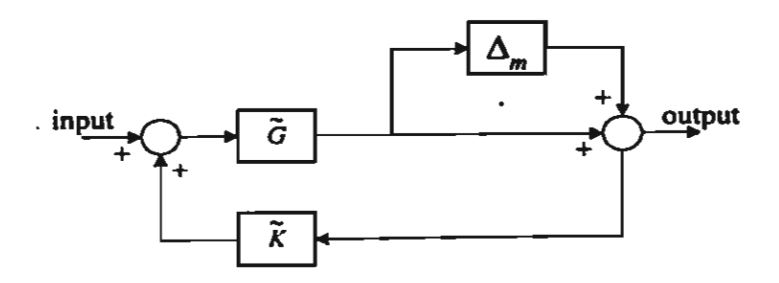


Figure 5. Control system with multiplicative uncertainty model

Based on the small-gain theorem [9-11], the closed loop system will be robustly stable if

$$\left|\Delta_{m}\right| < \frac{1}{\left|\tilde{G}\tilde{K}\left(1-\tilde{G}\tilde{K}\right)^{-1}\right|} \tag{15}$$

where  $\tilde{G}\tilde{K}\left(1-\tilde{G}\tilde{K}\right)^{-1}$  is the complementary sensitivity function (T). Note that  $|\bullet|$  is the magnitude of the transfer function " $\bullet$ ". Based on the multiplicative uncertainty model, the robust stability margin can be guaranteed in terms of multiplicative stability margin (MSM) as

$$MSM = 1/|T|$$
 (16)

where  $||T||_{r}$  is the  $\infty$ -norm of T. From (15) and (16), it is clear that by minimizing  $||T||_{x}$ , the MSM increases and the robust stability is ensured [9-11]. Thus, the normalized robustness index of the objective function is defined as

$$\gamma = \|T\|_{\tau} / \|T\|_{\text{attented}} \tag{17}$$

where  $||T||_{x(mual)}$  is the  $\infty$ -norm of T at the initial of a search process. Combining (14) and (17), the control problem can be formulated as the following optimization problem:

Minimize 
$$F(K, T_i) = c \cdot \alpha + \gamma$$
  
Subject to  $K_{\min} \leq K \leq K_{\max}$  (18)  
 $T_{i, \min} \leq T_i \leq T_{i, \max}, \quad i = 1, ..., 4$ 

where  $F(K, T_i)$  is the objective function. The minimum and maximum values of the gain K are set to 0.1 and 5, respectively. The minimum and maximum values of the time constants  $T_i$  are set to 0.01 and 2, respectively. The constant coefficient "c" is used to weight  $\alpha$ -term, so that  $c \cdot \alpha$  dominates  $\gamma$  during the parameters optimization. Note that, since  $\gamma$  is normalized to 1 at the initial solution, it is easy to find the value of c so that  $c \cdot \alpha$  is greater than 1. Eventually, the search process minimizes both terms until  $c \cdot \alpha$  meets the design specification and  $\gamma$  decreases to the possible minimum value. All searched parameters are optimized by a tabu search algorithm.

#### 3.6 Tabu Search Algorithm

Tabu Search (TS) is an iterative improvement procedure that can start from any initial feasible solution (searched parameters) and attempted to determine a better solution. As a meta-heuristic, TS is based on a local search technique with the ability to escape from being trapped in local optima [13, 14]. Hereafter, components of TS and TS procedure are discussed.

Encoding and Decoding: The concatenated encoding method is used to encode each parameter into a binary string normalized over its range and also stack each normalized string in series with each other to construct the string individual. The same number of *nb* bits is used for each searched parameter. Figure 6 illustrates the example of concatenated encoding scheme.

Figure 6. Example of Concatenated Encoding Scheme

On the other hand, a decoding scheme is carried out by converting encoded parameters to their actual values by (19) prior to evaluation of objective function.

$$P_i = P_{i,\min} + \frac{B_i \times \left[P_{i,\max} - P_{i,\min}\right]}{2^p - 1}$$
 (19)

where  $P_i$  is the actual value of the *i*-th parameter,  $P_{i,max}$  and  $P_{i,min}$  are the maximum and minimum value of the *i*-th parameter.  $B_i$  is the decimal integer value of binary string of the *i*-th parameter. In this study, 16 bits are used to represent each parameter. The more the number of bits per searched parameter is, the higher the resolution will be.

Trial Solution Generation. To generate a trial solution, one bit of a binary string of an initial solution is flipped at a time. Figure 7 conceptually illustrates the process. The maximum number of trial solutions in each iteration is referred to a neighborhood solution space (NS). In this paper, NS is set to  $90^{\circ}$  of a total number of bits in a string individual ( $\lfloor 0.9 \times nb \times NP \rfloor$  where NP is a number of searched parameters.

```
      Initial solution:
      1001011010
      1100011010
      1110010011

      Trial solution 1:
      2001011010
      1100011010
      1110010011

      Trial solution 2:
      1201011010
      1100011010
      1110010011

      Trial solution 3:
      1021011010
      1100011010
      1110010011
```

Figure 7 Example of Concatenated Encoding Scheme

Tabu List Restriction Tabu List (TL) is utilized to keep attributes (bit positions) that created the bound solution in the past iterations for iterations so that they can not be used to create new solution candidates. As the iteration proceeds, TL stores a new attribute and releases the oldest one, as shown in Fig. 8. Purticularly, the size of TL is the only control parameter of TS. The size of TL that provided good solutions usually grows with the size of the problem. In this paper,  $\lfloor \sqrt{nb \times NP} \rfloor$  is used to determine the best size of TL.

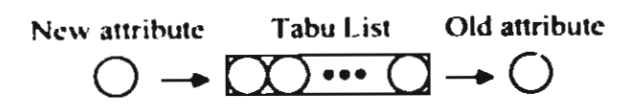


Figure 8. Mechanism of tabu list

Aspiration Level Criterion. The aspiration level (AL) criterion allows an attribute included in TL to override its tabu status if it leads to a more attractive solution. In particular, the AL is satisfied if the tabued attribute yields a solution that is better than the best solution reached at that iteration. After the AL is satisfied, updating TL is carried out by moving the tabued attribute back to the first position of the TL.

Termination Criteria. This criterion is set to allow the search process to stop and return the best solution found. The search process will terminate if the maximum allowable number of iterations is reached.

TS Procedure: firstly, the initial feasible solution is generated arbitrarily. A trial solution is searched if either it is not tabued or, in case of being tabued it passes the AL test. The best solution is always updated during the search process until the termination criterion is satisfied. The following notations are used for the TS procedure.

TL: the tabu list,

NS: the neighborhood solution space, F(X): the objective function of solution X,  $X_a^k$ : the initial feasible solution at iteration k,

 $X_{m}^{k}$ : a trial solution m at iteration k,

 $X_{cb}^{k}$ : the current best trial solution at iteration k, the best solution reached at iteration k,

the maximum allowable number of iterations.

The TS procedure can be described as follows.

- 1. Read constraints of searched parameters, the initial feasible solution  $X_n^{\lambda}$ , and the design specification.
- 2. Specify the size of TL,  $k_{min}$ , and size of NS.
- 3. Initialize iteration counter k and termination criteria te to zero, and empty TL.
- Initialized A1 by setting Λ<sup>\*</sup><sub>i</sub> · Λ<sup>\*</sup><sub>i</sub>.
- 5. Execute TS procedure:
  - 5.1 Initialize the trial counter m to zero.
  - 5.2 Generate a trial solution  $X_m^{(k)}$  from  $X_n^{(k)}$ .
  - 5.3 If  $X_m^A$  is not feasible, go to 5.9.
  - 5.4 If  $X_m^A$  is the first feasible solution, set  $X_{ch}^A = X_m^A$ .

  - 5.5 Perform Tabu test. If  $X_m^A$  is tabued, then go to 5.8. 5.6 If  $F(X_m^A) \sim F(X_h^A)$ , set  $X_h^A = X_m^A$ . Otherwise, go to 5.9. 5.7 If  $F(X_m^A) \sim F(X_h^A)$ , then update AL by setting  $X_h^A = X_m^A$ . Go to 5.9.
  - 5.8 Perform Al. test. If  $F(X_m^k) \le F(X_h^k)$ , set  $X_{i,h}^{k} \in \hat{X}_m^k$ , and update Al. by setting  $X_b^{k} = X_m^{k}$ .

  - 5.9 If m is less than NS, m = m+1 and go to 5.2. 5.10 If there is no feasible solution, set  $X_c^{(k-1)} \in X_b^{(k)}$ . Otherwise, set  $X_c^{(k-1)} = X_{cb}^{(k)}$ , and update
- If k = 0, go to 9.
- 7. Perform the convergence checking. If  $X_b^{\lambda} = X_b^{\lambda/I}$ , tc = tc + I. Otherwise, tc = 0.
- 8. If to size of TL, set to 0 and go to 10.
- 9. If  $k \leq k_{\text{max}}$ , then  $k = k \cdot 1$ , and go to 5.
- 10. TS is terminated and  $X_s^{A}$  is the best solution found.

## 4. Experimental Results

In the design specification, the desired damping ratio ( $\zeta_{desired}$ ) is set to 0.25. Also, the coefficient c is appropriately set to 5. For TS, the size of TL is set to 8 for the best solution. The area capacity ratio between areas 1, 2 and 3 is 5:10:2. System parameters are given in Table 1.

To exhibit the results of system reduction by overlapping decompositions, Table 2 shows eigenvalues of the original systems (1) in comparison to design subsystems (9) and (10). The damping ratio and oscillation frequency of the corresponding oscillation mode in the design subsystems are nearly equal to those of the original system. This reveals that the design subsystems (9) and (10) retain the physical characteristic of the original system (1).

As experimental results, the optimally tuned parameters of designed frequency stabilizers in (11) and (12) are obtained as given in Table 3. Note that the optimized frequency stabilizer based on (18) is referred to as "Robust frequency stabilizer".

For comparison purposes, the second-order lead/lag frequency stabilizer in (11) and (12) are also designed with the same design specification, which requires the same damping ratio  $\zeta_{desired} = 0.25$ . The control parameters  $K, T_1, T_2, T_3$ , and  $T_4$  are searched by TS via the optimization problem (20). Note that the robust stability index term  $(\gamma)$  is excluded.

Minimize 
$$F(K,T_i) = \alpha$$
  
Subject to  $K_{\min} \le K \le K_{\max}$  (20)  
 $T_{i,\min} \le T_i \le T_{i,\max}$ ,  $i = 1,...,4$ 

Here, the optimized frequency stabilizer based on (20) is referred to as "Non-robust frequency stabilizer". Table 4 shows the control parameters of the non-robust frequency stabilizer.

Table 1. Parameters of Three-area Loop Interconnected Power System (Area Capacity Ratio 5 : 10 : 2)

System Parameters	Area 1	Area 2	Area 3
Inertia Constant (pu.MW.s Hz)	$M_1 = 0.2$	$M_z = 0.0167$	$M_1 = 0.15$
Damping Coefficient (pu.MW/Hz)	$D_1 = 0.006$	$D_2 = 0.00833$	$D_{\rm j} = 0.005$
Turbine Time Constant (s)	$T_{i1}=0.25$	$T_{r_2} = 0.3$	$T_{r_3} = 0.25$
Governor Time Constant (s)	$T_{g1} = 0.1$	$T_{g2}=0.08$	$T_{g3}=0.1$
Regulation Ratio (Hz pu.MW)	$R_1 = 2.4$	$R_2 = 2.4$	$R_3 = 2.4$
Bias Coefficient (pu.MW Hz)	$B_1 = 0.5$	$B_2 = 0.5$	$B_{1} = 0.5$
Integral Controller Gain (1/s)	K , = 0.5	$K_{,2} = 0.5$	K,3 = 0.5
Synchronizing Power Coefficient (pu.MW/rad)	$T_{i2} =$	$0.159, T_{23} = 0.064, T_{31} = 0.064$	.079
Area Capacity Ratio ·	$a_{12} = 2.0$ , $a_{23} = 0.2$ , $a_{31} = 2.5$		

**Table 2.** Eigenvalues of Original System and Design Subsystems Before and After the Overlapping Decompositons

Original System (1)	Subsystem (11) ·	Subsystem (12)
$\lambda_1 = -0.0415$	-	-
$\lambda_{2,3} = -0.0173 \pm j4.365$	$\lambda_{2.3} = -0.015 \pm j3.53$	-
$(\zeta = 0.0035, f = 0.695 Hz)$	$(\zeta = 0.0043, f = 0.562 Hz)$	
$\lambda_{4,5} = -0.0185 \pm j3.291$	-	$\lambda_{4,5} = -0.0167 \pm j3.31$
$(\zeta = 0.0056, f = 0.524 Hz)$		$(\zeta = 0.005, f = 0.527 Hz)$

Table 3. Parameters of Robust Frequency Stabilizers

Robust Frequency					
Stabilizer	K	T <sub>i</sub>	<i>T</i> <sub>2</sub>	$T_3$	T,
SSSC12	0.2188	0.2587	0.0158	0.0575	0.2316
SSSC23	0.2378	1.5025	0.5386	1.6268	0.5075

Table 4. Parameters of Non-Robust Frequency Stabilizers

Non-robust Frequency					
Stabilizer	K	$T_{i}$	<i>T</i> <sub>2</sub>	<i>T</i> <sub>3</sub>	T <sub>4</sub>
SSSC12	4.2863	0.1344	1.0011	1.0978	1.3807
SSSC23	4.3683	0.1344	0.9933	1.3467	1.3802

Table 5. Comparison of Eigenvalues of Design Subsystems

Design Subsystem	SSSC with No Frequency Stabilizer	SSSC With Non- Robust Frequency	SSSC With Robust Frequency
		Stabilizer	Stabilizer
$G_{\mathfrak{sl}}$	$-0.015 \pm j3.53$	$-1.8369 \pm j7.1143$	$-0.6093 \pm j2.3595$
	$\zeta = 0.0043$	$\zeta = 0.25$	$\zeta = 0.25$
$G_{i2}$	$-0.0167 \pm j3.31$	$-1.667 \pm j6.4559$	$-0.3534 \pm j1.3685$
	$\zeta = 0.005$	ζ = 0.25	$\zeta = 0.25$

Table 5 shows eigenvalues of subsystems (11) and (12) in case of SSSCs with robust frequency stabilizers installed in comparison with a case of SSSCs with no frequency stabilizer and a case of SSSCs with non-robust frequency stabilizers installed. The results describe that the damping ratios of the eigenvalues corresponding to the desired inter-area modes are improved to 0.25, as design specification.

Next, the MSM is used to evaluate the robust stability margin of system (11) and (12) included with each frequency stabilizer. As shown in Table 6, the value of MSM in case of the system with robust frequency stabilizer is greater than that in case of the system with non-robust stabilizer. This clearly signifies that the better robust stability margin of the power system incorporated with robust frequency stabilizer can be achieved by the optimization problem (18).

Table 6. Comparison of MSM

System	With Non-Robust Frequency Stabilizer	With Robust Frequency Stabilizer
$G_{N1}$	0.5151	0.71430
$G_{N2}$	0.5332	0.61240

Table 7. Comparison of Eigenvalues of Original System

Inter-Area Oscillation  Mode	No Frequency Stabilizer	With Non-Robust Frequency Stabilizer	With Robust Frequency Stabilizer
Between Areas	$-0.0173 \pm j4.365$	$-1.7631 \pm j7.6011$	-0.6619 ± j2.898
1 and 2	$\zeta = 0.0035$	$\zeta = 0.226$	$\zeta = 0.223$
Between Areas	$-0.0185 \pm j3.291$	-1.6716 ± j6.4702	$-0.3596 \pm j1.376$
2 and 3	$\zeta = 0.0056$	$\zeta = 0.25$	$\zeta = 0.253$

Table 7 shows the eigenvalues of the original system (1) before and after control. After each frequency stabilizer is included in the system, the damping ratios of the corresponding inter-area modes are enhanced as expected. This confirms the merit of overlapping decompositions that if the subsystems are stabilized by their own control inputs, the stability of the original system can be guaranteed.

Here, the performance and robustness of the designed frequency stabilizers are evaluated in a linearized model of the three-area interconnected system. Here, changing load disturbances which are simultaneously applied to areas 1 and 3, are composed of three different components in the frequency domain, one of which (underlined component) has a frequency corresponding to the inter-area mode of interest (see Table 6), as follows.

Area 1: 
$$\Delta P_{L1} = 0.003\sin(4.36t) + 0.005\sin(5.3t) - 0.007\sin(6t)$$
 (21)

Area 3: 
$$\Delta P_{t,t} = 0.003\sin(3.29t) + 0.007\sin(4t) - 0.005\sin(4.5t)$$
 (22)

Note that the dynamic of governor as illustrated in Fig. 9, is also included into each area in this simulation study. Table 8 shows operating conditions and applied disturbances.

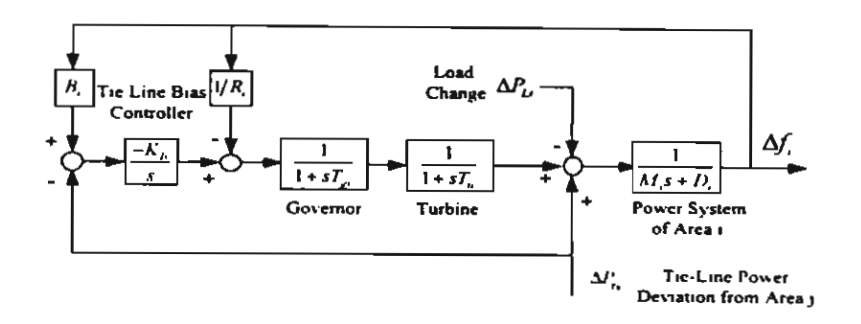


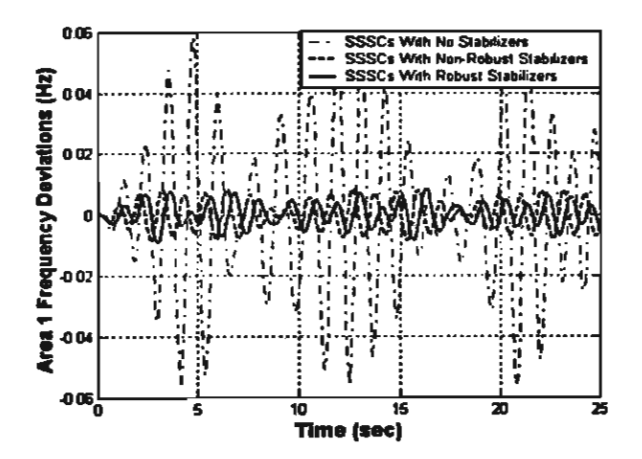
Figure 9. Linearized model of governor system

Table 8. System Conditions and Applied Disturbances

Case	Disturbances
1	At normal (design) condition, $\Delta P_{L1}$ is applied to area 1 and $\Delta P_{L3}$ is
	applied to area 3. (No parameter variations)
2	At unstable condition, $\Delta P_{L1}$ is applied to area 1 and $\Delta P_{L3}$ is applied
	at area 3 while damping coefficients $D_1$ and $D_3$ are set -0.45.

For case 1, the damping effect of each designed stabilizer is investigated. As demonstrated in Figs. 10 – 12, both robust and non-robust frequency stabilizers are able to damp the frequency oscillation in each area, effectively. Nevertheless, the damping effect of the robust frequency stabilizer is better than that of the non-robust case. As declared in Figs. 13 and 14, the power output deviation of the robust frequency stabilizer for each SSSC is almost equal to that of non-robust frequency stabilizer.

In case 2, not only damping effect but also robust stability of the system incorporated with each frequency stabilizer are evaluated. It is assumed that both power systems 1 and 3 are in unstable conditions, so that  $D_1$  and  $D_3$  are set to -0.45 (pu.MW/Hz). As the load disturbances applied to both areas, frequency deviations of areas 1, 2 and 3 in case of the non-robust frequency stabilizer severely fluctuate and finally diverge as depicted in Figs. 15–17. Note that frequency deviation of each area in case of SSSCs without frequency stabilizers (not shown here) also heavily oscillates and finally diverges. On the other hand, frequency oscillations in all areas are completely stabilized by the robust frequency stabilizer. The interconnected power system can maintain the system stability. The power output deviations of robust frequency stabilizers are illustrated in Figs. 18 and 19. These simulation results confirm that under severe load disturbances and negative damping, the robustness of robust frequency stabilizer against such system uncertainties is considerably superior to that of non-robust frequency stabilizer.



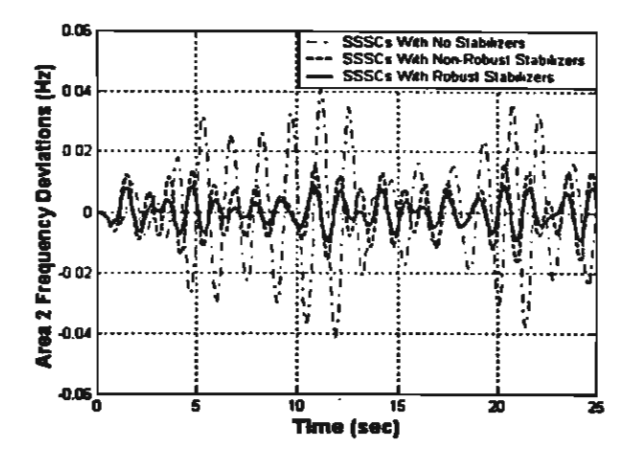


Figure 10. Case 1: Area 1 Frequency Deviation

Figure 11. Case 1: Area 2 Frequency Deviation

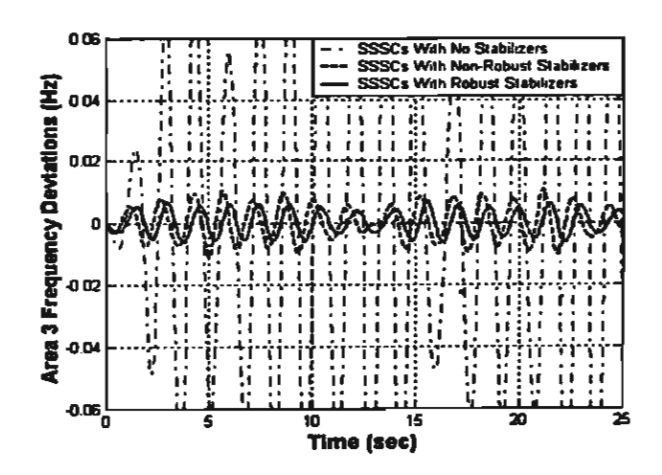


Figure 12. Case 1: Area 3 Frequency Deviation

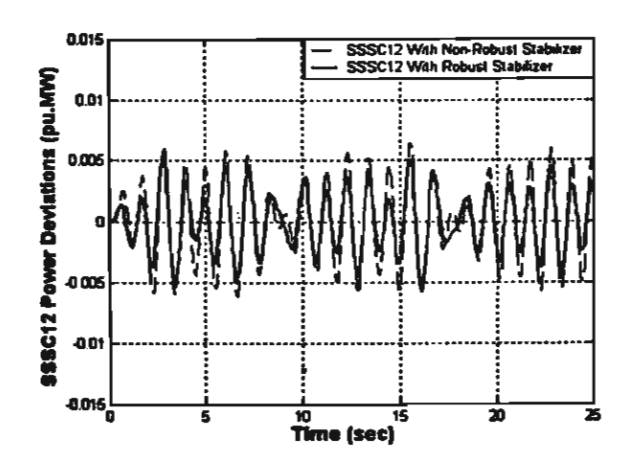


Figure 13. Case 1: SSSC12 Power Output

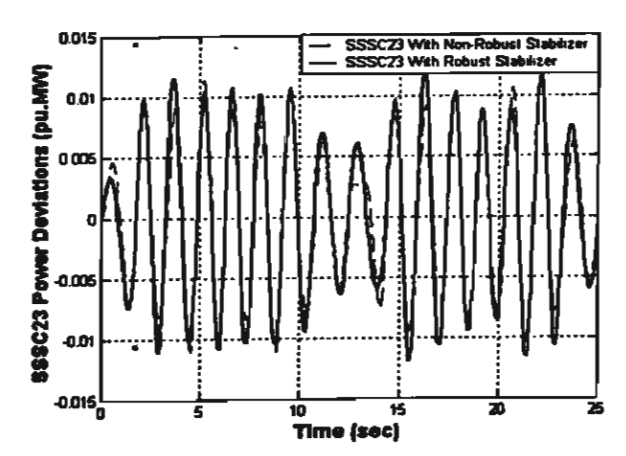
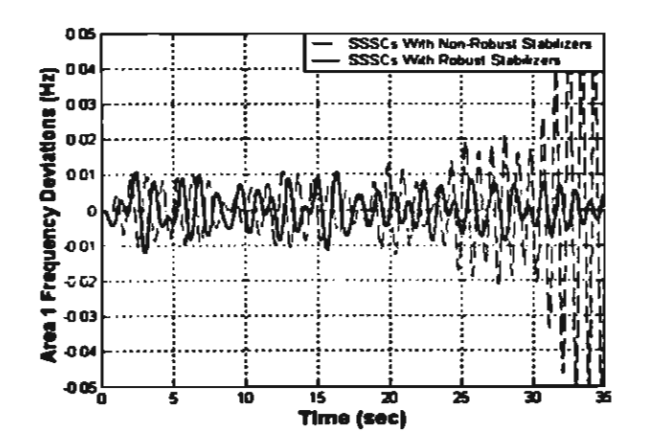


Figure 14. Case 1: SSSC23 Power Output



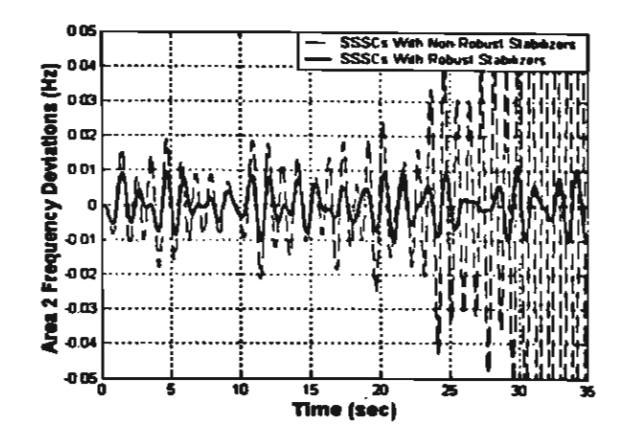


Figure 15. Case 2: Area 1 Frequency Deviation

Figure 16. Case 2: Area 2 Frequency Deviation

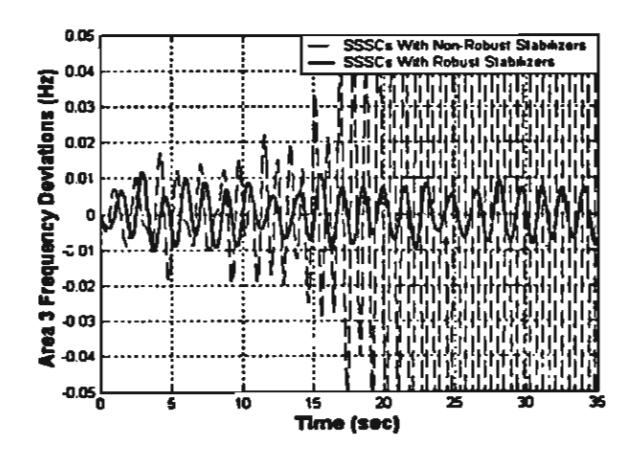


Figure 17. Case 2: Area 3 Frequency Deviation

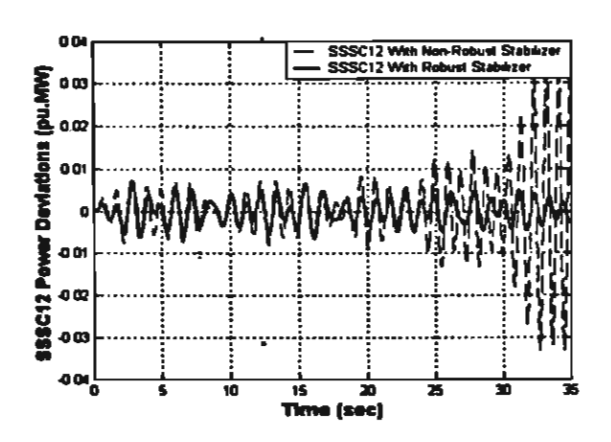


Figure 18. Case 2: SSSC12 Power Output

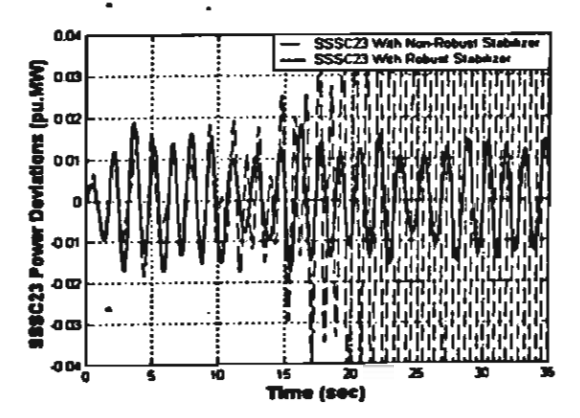


Figure 19. Case 2: SSSC23 Power Output

#### 5. Conclusions

This paper focuses on the new robust design of frequency stabilizer of SSSC by taking system uncertainties into account. The design method utilizes the merit of overlapping decompositions technique to extract the subsystem embedded with the inter-area oscillation mode of interest. By including the multiplicative uncertainty model in the extracted subsystem, the robust stability index based on multiplicative stability margin can be applied in the formulation of objective function. As a result, the robust stability margin of system with designed frequency stabilizer can be enhanced by optimization technique. Without trial and error, the tabu search algorithm is automatically applied to search for the optimal control parameters of the second-order lead/lag based frequency stabilizer. The high robustness of the designed frequency stabilizer against various load disturbances with changing frequency in the vicinity of inter-area mode and negative damping, has been confirmed by simulation study.

#### 6. Reference

- 1. F. D. Galliana and M. Illic, Power System Restructuring, Kluwer Academic Publishers, 1998.
- 2. K. N. Zadeh, R. C. Meyer and G. Cauley, Practices and new concepts in power system control, *IEEE Trans. on Power Systems* 11 (1) (1996) 3-9.
- 3. L. H. Fink and P. J. M. Van Son, On system control within a restructured Industry, *IEEE* Trans. on Power Systems, 13 (2) (1998) 611-616.
- 4. O.L. Elgerd, Electric Energy System Theory, An Introduction 2nd, McGraw-Hill, 1985.
- 5. N. Jaleeli, L.S. Vanslyck, D.N. Ewart, L.H. Fink and A.G. Hoffmann, Understanding automatic generation control, *IEEE Transactions on Power Systems*, Vol. 7, No. 3, pp. 1106-1122, 1999.
- 6. I. Ngamroo, Application of static synchronous series compensation to stabilization of frequency oscillations in an interconnected power system, *Proceedings of 2001 IEEE International Symposium on Circuits and Systems (ISCAS 2001), Sydney, Australia*, Vol. 2, pp. 113-116.
- 7. L. Gyugyi, Dynamic compensator of AC transmission lines by solid-state synchronous voltage source, *IEEE Trans. on Power Delivery*, Vol. 9, No. 2, pp. 904-911, 1994.
- 8. L. Gyugyi, C. D. Schauder and K.K. Sen, Static Synchronous Series Compensator: A Solid-State Approach to The Series Compensation of Transmission Lines, *IEEE Trans. on Power Delivery*, Vol. 12, No. 1, pp. 406-417, 1997.
- 9. S. Skogestad and I. Postlethwaite, Multivariable Feedback Control, Analysis and Design, John Wiley & Sons, 1998.
- 10. G. C. Goodwin, S. F. Graebe and M. E. Salgado, Control System Design, Prentice Hall, 2001.
- 11. B. Shahian and M. Hassul, Control System Design using MATLAB, Prentice Hall, 1993.
- 12. M. Ikeda, D.D. Siljak and D. E. White, Decentralized control with overlapping information sets. Journal of Optimization Theory and Applications, Vol. 34, No. 2, pp.279-310, 1981.
- 13. F. Glover and M. Laguna, Tabu Search, Kluwer Academic Publishers, 2000.
- 14. V. J. Rayward-Smith, I. H. Osman, C.R. Reeves, and G.D. Smith, *Modern Heuristic Search Methods*, John Wiley & Sons, UK, 1996.
- 15. P. Kundur, Power System Stability and Control, McGraw Hill, 1994.